

PHYSICO-CHEMICAL CHARACTERIZATION OF CEMENT TYPE  
HYDRATION OF ALPHA-TRICALCIUM PHOSPHATE

A THESIS SUBMITTED TO  
THE GRADUATE SCHOOL OF NATURAL AND APPLIED SCIENCES  
OF  
MIDDLE EAST TECHNICAL UNIVERSITY



BY  
MEHMET YİĞİT KÖHNETARFUN

IN PARTIAL FULFILLMENT OF THE REQUIREMENTS  
FOR  
THE DEGREE OF MASTER OF SCIENCE  
IN  
METALLURGICAL AND MATERIALS ENGINEERING

DECEMBER 2024



Approval of the thesis:

**PHYSICO-CHEMICAL CHARACTERIZATION OF CEMENT TYPE  
HYDRATION OF ALPHA-TRICALCIUM PHOSPHATE**

submitted by **MEHMET YİĞİT KÖHNETARFUN** in partial fulfillment of the requirements for the degree of **Master of Science in Metallurgical and Materials Engineering, Middle East Technical University** by,

Prof. Dr. Naci Emre Altun  
Dean, Graduate School of **Natural and Applied Sciences** \_\_\_\_\_

Prof. Dr. Ali Kalkanlı  
Head of Department, **Metallurgical and Materials Engineering** \_\_\_\_\_

Prof. Dr. Caner Durucan  
Supervisor, **Metallurgical and Materials Engineering, METU** \_\_\_\_\_

**Examining Committee Members:**

Prof. Dr. Arcan F. Dericioğlu  
Metallurgical and Materials Engineering, METU \_\_\_\_\_

Prof. Dr. Caner Durucan  
Metallurgical and Materials Engineering, METU \_\_\_\_\_

Prof. Dr. Ziya Esen  
Inter-Curricular Courses Department, Çankaya University \_\_\_\_\_

Assist. Prof. Dr. Irmak Sargin  
Metallurgical and Materials Engineering, METU \_\_\_\_\_

Assist. Prof. Dr. Yusuf Keleştemur  
Metallurgical and Materials Engineering, METU \_\_\_\_\_

Date: 02.12.2024



**I hereby declare that all information in this document has been obtained and presented in accordance with academic rules and ethical conduct. I also declare that, as required by these rules and conduct, I have fully cited and referenced all material and results that are not original to this work.**

Name Last name : Mehmet Yiğit Köhnetarfun

Signature :

## ABSTRACT

### PHYSICO-CHEMICAL CHARACTERIZATION OF CEMENT TYPE HYDRATION OF ALPHA-TRICALCIUM PHOSPHATE

Köhnetarfun, Mehmet Yiğit  
Master of Science, Metallurgical and Materials Engineering  
Supervisor : Prof. Dr. Caner Durucan

December 2024, 68 pages

Synthetic bone grafts are widely employed in bone restoration procedures, particularly in the treatment of bone defects. Alpha-tricalcium phosphate ( $\alpha$ -TCP,  $\alpha$ - $\text{Ca}_3(\text{PO}_4)_2$ ) is a commonly utilized calcium orthophosphate material for bone filling applications. Upon hydration with aqueous solutions,  $\alpha$ -TCP-based powder cement systems undergo a transformation into calcium-deficient hydroxyapatite (CDHAp,  $\text{Ca}_9(\text{HPO}_4)(\text{PO}_4)_5(\text{OH})$ ), a key inorganic component of bone tissue that plays a critical role in bone healing and defect regeneration. The primary objective of this thesis is to synthesize pure  $\alpha$ -TCP powder through a solid-state reaction, followed by detailed evaluation of its hydration behavior/reactivity under various-reaction conditions. The investigation aims to identify the optimal parameters by assessing the transformation of the cement in terms of its microstructural and mechanical properties. The parameters including—solid-to-liquid ratio of cement mixture, hydration temperature, hydration time, and hydration media were systematically studied. The experimental investigations were conducted using x-ray diffraction, electron microscopy, and mechanical testing to assess the effects of these variables. Specifically, the impact of temperature on hydration was examined at 25°C, 37°C, and 60°C. To explore the effect of the solid-to-liquid ratio, ratios of 1:1, 1:3, and 1:5

were tested. The effect of hydration time was evaluated at intervals of 1 hour, 4 hours, 8 hours, 12 hours, 24 hours, and 56 hours. Additionally, disodium phosphate ( $\text{Na}_2\text{HPO}_4$ ) solutions were employed together with DI-water, to investigate the influence of the hydration media on cement conversion. The results demonstrated that the addition of  $\text{Na}_2\text{HPO}_4$  significantly accelerated the  $\alpha$ -TCP to CDHAp transformation; however, it concurrently led to a reduction in fracture strength.

Key words: Tricalcium Phosphate, Bone Fillers, Calcium Deficiency  
Hydroxyapatite



## ÖZ

### ALFA-TRİKALSİYUM FOSFATIN ÇİMENTO TİPİ HİDRASYONUNUN FİZİKO-KİMYASAL KARAKTERİZASYONU

Köhnetarfun, Mehmet Yiğit  
Yüksek Lisans, Metalurji ve Malzeme Mühendisliği  
Tez Yöneticisi: Prof. Dr. Caner Durucan

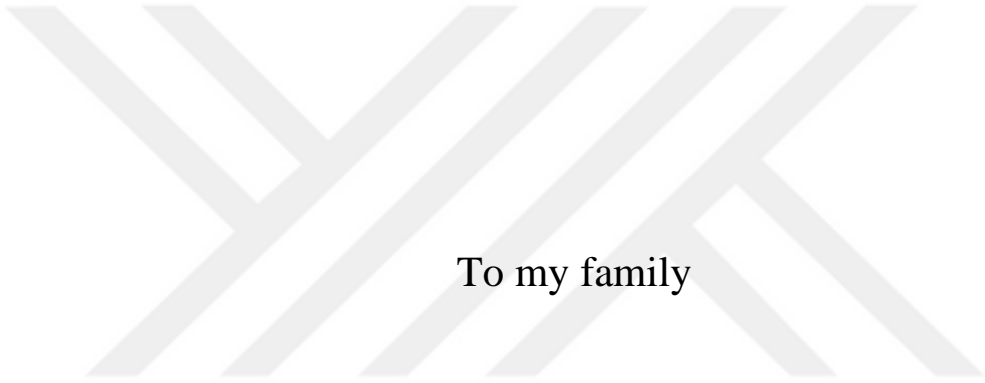
Aralık 2024, 68 sayfa

Sentetik kemik greftleri, özellikle kemik defektlerinin tedavisinde, kemik restorasyon prosedürlerinde yaygın olarak kullanılır. Alfa-trikalsiyum fosfat ( $\alpha$ -TCP,  $\alpha$ -Ca<sub>3</sub>(PO<sub>4</sub>)<sub>2</sub>), kemik dolgu uygulamaları için yaygın olarak kullanılan bir kalsiyum ortofosfat malzemesidir. Sulu çözeltilerle nemlendirildiğinde,  $\alpha$ -TCP bazlı toz çimento sistemleri, kemik iyileşmesinde ve defekt rejenerasyonunda kritik bir rol oynayan kemik dokusunun önemli bir inorganik bileşeni olan kalsiyum eksikliği olan hidroksiapatite (CDHAp, Ca<sub>9</sub>(HPO<sub>4</sub>)(PO<sub>4</sub>)<sub>5</sub>(OH)) dönüşür. Bu tezin birincil amacı, katı hal reaksiyonu yoluyla saf  $\alpha$ -TCP tozunu sentezlemek ve ardından çeşitli reaksiyon koşulları altında nemlendirme davranışının/reaktivitesinin ayrıntılı bir şekilde değerlendirilmesidir. Araştırma, çimentonun mikro yapısal ve mekanik özellikleri açısından dönüşümünü değerlendirerek optimum parametreleri belirlemeyi amaçlamaktadır. Çimento karışımının katı-sıvı oranı, hidrasyon sıcaklığı, hidrasyon süresi ve hidrasyon ortamı gibi parametreler sistematik olarak incelenmiştir. Deneysel araştırmalar, bu değişkenlerin etkilerini değerlendirmek için x-ışını kırınımı, elektron mikroskobu ve mekanik testler kullanılarak yürütülmüştür. Özellikle, sıcaklığın hidrasyon üzerindeki etkisi 25 °C, 37 °C ve 60 °C'de incelenmiştir. Katı-sıvı oranının etkisini araştırmak için 1:1, 1:3 ve 1:5 oranları test edilmiştir. Hidrasyon süresinin etkisi 1 saat, 4 saat, 8 saat, 12 saat,

24 saat ve 56 saatlik aralıklarla deęerlendirilmiřtir. Ek olarak, hidrasyon ortamının imento donşümü üzerindeki etkisini arařtırmak iin disodyum fosfat ( $\text{Na}_2\text{HPO}_4$ ) zelteleri DI-su ile birlikte kullanılmıřtır. Sonular,  $\text{Na}_2\text{HPO}_4$  ilavesinin  $\alpha$ -TCP'den CDHAp'ye donřmünü önemli ölçüde hızlandırdığını; ancak aynı zamanda kırılma dayanıklılıęında bir azalmaya yol atıęını göstermiřtir.

Anahtar kelimeler: Trikalsiyum Fosfat, Kemik Dolguları, Kalsiyum Eksiklięi Olan Hidroksiapatit





To my family

## ACKNOWLEDGMENTS

I would like to convey my heartfelt gratitude to my supervisor, Prof. Dr. Caner Durucan, for his invaluable supervision, patience, encouragement, guidance and support not only throughout this thesis but in many other studies.

I would like to thank Dr. Hakan Yavaş for his advice, guidance, support and for helping me get my master's degree.

I would like to thank all my lab mates and the Department of Metallurgical and Materials Engineering for their support.

I would also like to thank my dear girlfriend Merve Özgür for constantly improving me, making me more productive and successful, not only during my graduate studies but also since the day we met.

Finally, I am very grateful to my mother, father and sister for their unconditional support, love and always being there for me throughout my life. I am very lucky to have such a wonderful family.

## TABLE OF CONTENTS

ABSTRACT.....	v
ÖZ .....	vii
ACKNOWLEDGMENTS .....	x
TABLE OF CONTENTS.....	xi
LIST OF TABLES .....	xiii
LIST OF FIGURES .....	xiv
LIST OF ABBREVIATIONS .....	xvi
CHAPTERS	
1 INTRODUCTION .....	1
2 LITERATURE REVIEW .....	3
2.1 Composition, structure and properties of natural bone .....	3
2.2 Bioceramics .....	7
2.3 Natural Bone Grafts .....	9
2.4. Synthetic Bone Grafts.....	10
2.5. Objective and general structure of the thesis.....	19
3 MATERIALS AND METHODS.....	23
3.2.1. Preparation of Monetite (CaHPO <sub>4</sub> ): Solid reactant for α-TCP.....	25
4 RESULTS and DISCUSSIONS.....	31
4.1 Characterization of Monetite Powders .....	31
4.2 Characterization of α-TCP Powders.....	32
4.2.1 XRD Characterization of α-TCP Powders.....	32
4.2.2 SEM Characterization of α-TCP Powders .....	33
4.3 Evaluation of hydration behavior of α-TCP: Effect of solid:liquid ratio .	34

4.4	Evaluation of hydration behavior of $\alpha$ -TCP: Hydration/reaction kinetics	39
4.5	Evaluation of hydration behavior of $\alpha$ -TCP: Hydration temperature	43
4.6	Evaluation of hydration behavior of $\alpha$ -TCP: Hydration media (Na <sub>2</sub> HPO <sub>4</sub> ) <sub>aq</sub>	47
4.7	Evaluation of cement hardening: Mechanical testing	52
5	CONCLUSIONS	55
	REFERENCES	59



## LIST OF TABLES

### TABLES

Table 2.1 Calcium phosphate varieties with solubility, Ca/P molar ratio and pH stability properties.....	13
--	----



## LIST OF FIGURES

### FIGURES

Figure 2.1 The hierarchical level in bone structure by scaling.....	4
Figure 2.2 Schematic illustration of collagen fibrils, fibers and bone mineral crystals in nanoscale.....	5
Figure 2.3. Solubility isotherms for various calcium phosphate compounds in aqueous media, depending on pH levels.....	14
Figure 2.4. The rational planning and outline of the thesis.....	20
Figure 3.1. Synthesis details of $\alpha$ -TCP including the chemical reactions leading to formation of intermediate reactants and final product $\alpha$ -TCP.....	24
Figure 3.2 Schematic representation of diametral compression test.....	29
Figure 4.1. XRD Diffractogram for the product of Monetite.....	32
Figure 4.2. XRD diffractograms of $\alpha$ -TCP powder.....	33
Figure 4.3. SEM micrograph for the product of $\alpha$ -TCP.....	34
Figure 4.4. XRD diffractograms of $\alpha$ -TCP powder, hydrated at different solid to liquid ratio (1:1, 1:3, 1:5) for 24 hours.....	36
Figure 4.5. SEM micrographs of the product phase resulting from $\alpha$ -TCP hydration for 24 hours, with a s:l ratio of 1:1, 1:3, 1:5, respectively (from top to bottom).....	38
Figure 4.6. XRD diffractograms for the end product of hydration $\alpha$ -TCP at 37°C with different reaction time. The solid:liquid ratio was of 1:3, and DI-water was the hydration media. ....	40
Figure 4.7 SEM micrographs of the product phase resulting from $\alpha$ -TCP hydration at 37 °C with DI-water, for 12, 24, 56, hours respectively; (from top to bottom) with a s:l ratio of 1:3.....	42

Figure 4.8 XRD diffractograms for hydrated products resulting from $\alpha$ -TCP hydration with DI-water for 24 hours at 25, 37, 60 °C, respectively, with a s:l ratio of 1:3. ....	44
Figure 4.9 SEM micrographs of the product phase resulting from $\alpha$ -TCP hydration with DI-water for 24 hours at 25, 37, 60 °C, respectively,(from top to bottom), with a s:l ratio of 1:3.....	46
Figure 4.10. XRD diffractograms for hydrated products resulting from $\alpha$ -TCP hydration in % Na <sub>2</sub> HPO <sub>4</sub> solutions (1.0 wt %,2.5. wt% and 5.0 wt% ) at 37°C....	49
Figure 4.11. SEM micrographs of the product phase resulting from $\alpha$ -TCP hydration with Na <sub>2</sub> HPO <sub>4</sub> solutions 1.0 wt %,2.5. wt% and 5.0 wt% respectively (from top to bottom) at 37°C for 24 hours.....	51
Figure 4.12. Mechanical properties of pure $\alpha$ -TCP and $\alpha$ -TCP pellets hydrated with DI water and Na <sub>2</sub> HPO <sub>4</sub> solutions, at varying solid-to-liquid ratios, at 37°C for 24 hours. ....	52

## LIST OF ABBREVIATIONS

### ABBREVIATIONS

$\alpha$ -TCP	alpha-tricalcium phosphate
HAp	hydroxyapatite
CDHAp	calcium-deficient hydroxyapatite
$\beta$ -TCP	beta-tricalcium phosphate
CaP	calcium phosphate
CPC	calcium phosphate cement

# CHAPTER 1

## INTRODUCTION

Many different types of materials can be used in contemporary biomedical applications. The main groups of these materials are ceramics, metals and polymers. These materials are used for various purposes. Some of these are bone implants, filling and restorative materials in fractures that may occur after injuries and traumas. A key concern in designing these materials is ensuring that they are biocompatible and possess structural and mechanical properties that closely match those of natural bone.

Historically, Trauma and fractures may occur in the bone structure due to external factors, tumors may form due to diseases, or aging may occur in the bone over time. For these reasons, wear and tear and gaps occur in the bone structure. Natural or synthetic bone cements are used as filling materials to cover these damages. However, obtaining bone fillers from patients or donors can be inconvenient and limited by time, with additional risks such as disease transmission from donors. As a solution to the mentioned problems, bone cements have been developed and these materials are synthetic and biocompatible. The developed synthetic bone cements are turned into paste form and used on the bone in this way during medical procedures or surgeries.

Due to their biocompatibility, ceramic-based calcium phosphate cements also serve as a highly functional synthetic analogue due to their similarity to the mineral phase found in natural bone structure.

In addition, the hardening process of calcium phosphate cements (CPCs) is more compatible with physiological conditions than the polymerization-based hardening of acrylic polymers. CPCs are produced by combining calcium phosphate powders

with a liquid, resulting in a paste that sets and solidifies after being implanted in the body.

Calcium phosphate cements primarily produce two types of end products: apatite and brushite cements, with the latter being created by reacting an acidic calcium phosphate powder with a standard one in liquid solution to form a neutral cement. Apatite cements take on a hardened form when mixed with water or aqueous media. Their chemical similarity to the mineral phase of bone, which is biological apatite, is also one of the reasons for preference. It is also produced from alpha tricalcium phosphate. When hydrated, it can turn into hydroxyapatite, which is deficient in calcium.

## CHAPTER 2

### LITERATURE REVIEW

#### 2.1 Composition, structure and properties of natural bone

Bone is a structure composed of mineralized tissue and its primary function is to provide support for carrying loads. Bone is a composite material and consists of 3 main components, organic matrix, mineral and water. If the weight ratios of these 3 components are compared, the mineral part is the highest, 69%, organic matrix 20% and water 9%. The remaining 2% consists of living cells. These specific cells are osteoblasts, osteoclasts and osteocytes. [1]

While examining lamellar bone, Weiner and his team are testing the structure of this bone on two different materials, regular and irregular. This grouping is determined as regular material and irregular material. [2,3,4]

First, regular material is defined as mineralized collagen fibril and it is emphasized that this is the basic component of bone. This fibril in question is supported by the matrix in the collagen structure. Irregular material has collagen fibrils that are not regularly oriented and consists of mineral matrix. [5]

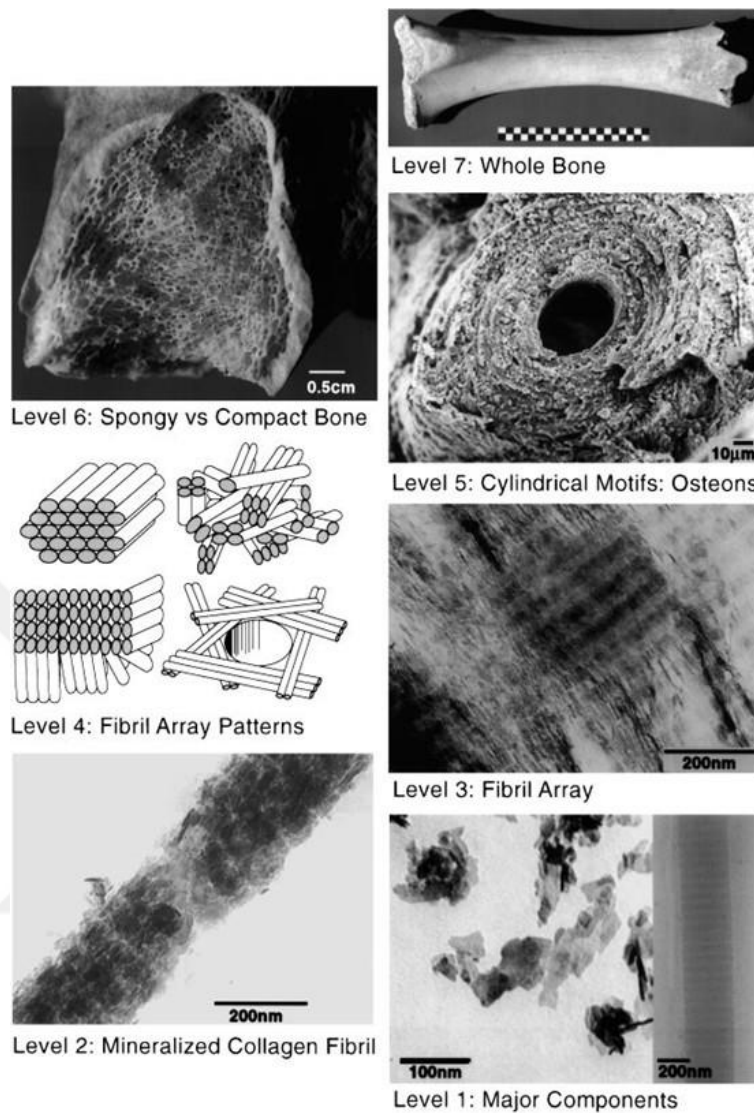


Figure 2.1 shows the hierarchical level in bone structure by scaling. [2].

There are many proteins that make up the organic component in the bone structure. The majority of this organic part is type 1 collagen proteins. The remaining 10% is made up of non-collagen proteins. Proteins called type 1 collagen are found in the bone structure as fibrils and their sizes vary between approximately 80-100 nm. [6]

Each fibril consists of three polypeptide chains, each about 1000 amino acids long, which coil together to form a triple helix. This helix has a cylindrical shape with a diameter of roughly 1.5 nm and a length of 300 nm, and features a periodicity of 67 nm. [6,7,8]

The spaces between these fibrils facilitate mineralization by allowing surrounding biological fluids to penetrate. These fibrils are organized into arrays, forming fiber structures. [9,10,] A detailed representation of the collagen structure and its dimensions is shown in the image with figure number 2.2.

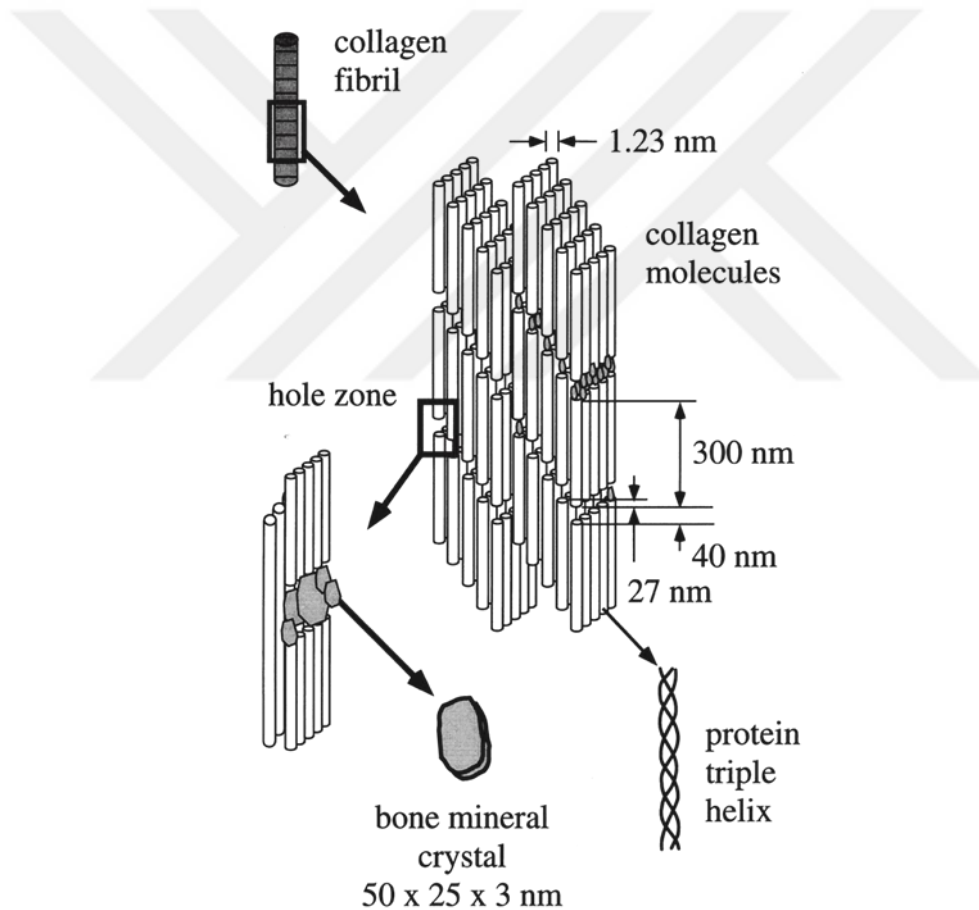


Figure 2.2 Schematic illustration of collagen fibrils, fibers and bone mineral crystals in nanoscale [11].

Nanosized crystals of biological apatite are called dahllites. Dahllites are structures that form the mineral composition of natural bone together with various ions such as magnesium, sodium, hydrogen phosphate and potassium. These nanocrystal structures are plate-shaped and have dimensions of approximately 50nm x 25nm x 3nm.[2,11,12] The primary functions of the mineral component are to serve as a source of ions and regulate their concentrations. Additionally, the integration of the mineral component with the organic matrix forms a composite structure that imparts exceptional toughness and lightness to the bone.[13,14]

Bone mineral has the formula  $\text{Ca}_{(10-x-y)}(\text{HPO}_4)_x(\text{CO}_3)_y(\text{PO}_4)_{(6-x-y)}(\text{OH})_{(2-x-y)}$  and consists of a carbonated apatite with a Ca/P ratio of less than 1.67. ( $0 < x, y < 1$ )

This is due to the trace amounts of different ions found in the mineral composition of the bone, its crystal size and morphology. For this reason, it differs from hydroxyapatite stoichiometrically and even in terms of the Ca/P ratio.[13]

According to Wilson and the working team, water in the bone structure is seen as an important material on the mineral surface. It has two important roles. It helps protect the bone from deformation by facilitating minimal movement between the bone mineral and collagen layer, thus providing structural stability. Additionally, water movement helps safeguard collagen from shear stress under uniaxial stress, preserving the integrity of the collagen. [14]

In addition, water can be found in the bone structure, inside the fibers and in the empty spaces between the fibers, on the bone mineral surface and between the spiral structures. [2]

Bone has the ability to repair and regenerate small cracks and damages on its own. The Haversian channels surrounding the osteons, derived from collagen lamellar sheets, acting as a depot by containing phosphate ions and calcium ions. This reservoir supports the dynamic remodeling of monocrystalline apatite through the action of osteoclasts and osteoblasts. [15] However, bone cannot heal fractures resulting from trauma, tumor removal, or age-related issues on its own. Natural or

synthetic bone grafts are used in these cases to help heal bone that has been worn down due to trauma or aging.

## **2.2 Bioceramics**

Ceramics that facilitate bond formation between structures such as bone and dental hard tissues, and possess the ability to form apatite, are referred to as bioceramics.[16]

Bioceramics are materials that occur naturally. Examples of natural sources include nacre, animal bones, and sponges, among others.[17] Additionally, bioceramics can be produced synthetically as well as through natural processes. This production involves high-temperature sintering and is characterized by enhanced mechanical properties and resistance to chemical corrosion.[18,19] While these materials provide benefits in terms of biocompatibility, they also have limitations related to mechanical properties, including brittleness, low elasticity, and high stiffness. [17]

Bioceramics can be categorized into two main groups: bioinert and bioactive. Bioactive bioceramics are further divided into two subcategories: resorbable and non-resorbable. [17] In terms of mechanical properties, alumina and zirconia represent the first generation of bioceramics, while bioactive glass, hydroxyapatite, and calcium phosphate-based cements comprise the second generation of bioceramics.[18,20] Bioceramics that incorporate absorbable proteins, which facilitate the regeneration of living cells and provide growth factors by functioning as a scaffold, are classified as third generation bioceramics. [21]

Bioceramics can be classified based on origin, tissue response, composition, and crystallinity.

Ceramic materials play a crucial role in medical applications, and various implants have been developed and implemented to replace or repair damaged or dysfunctional body parts. The initial applications of bioceramics focused on the treatment of dental issues and bone repair. These early uses laid the groundwork for further advancements in bioceramic technology and its integration into various medical implants. [21,22] Bioceramics, used to restore the fundamental functions of damaged bone, have advanced the field of tissue engineering. This progress is attributed to the fact that natural bone consists of living tissues, enabling the successful application of biomaterials to facilitate live bone development through tissue replacement. [23,24]

The general applications of bioceramics, including their use in soft tissue repairs, are highlighted in clinical studies.

Bioceramics provide numerous benefits to living organisms; however, complete compatibility with the structure of living tissues should not be expected. There are several challenges associated with the use of bioceramics. Developing these materials is a complex process, and maintaining their mechanical properties and biocompatibility at desired levels poses significant difficulties. Powdered materials, nanofilms, scaffolds, and bioceramics—collectively referred to as biomaterials—whether used individually or in combination, must be acceptable with the human body. The reasons for the rejection of bioceramics within the living body are being explored using various techniques and advancing technologies. However, due to the numerous dynamic parameters present in biological systems, these evaluations face significant challenges. To evaluate the compatibility of bioceramics with living tissues in both in vitro and in vivo settings, a variety of tests, especially cytotoxicity assessments, are performed on cell cultures and animal models. [25]

### 2.3 Natural Bone Grafts

Natural bone grafts fall into three categories: xenografts, allografts, and autografts. Xenografts involve transplanting grafts between different species. However, the use of xenografts is limited. The main reasons for this are the high probability of infection in the living being used and the low osteogenic properties. In addition, high absorption rates are another reason that limits their use. Allografts, on the other hand, are grafts transferred between individuals of the same species. However, their areas of use are low, like xenografts. The main reason for this is that they cause viral infections in the living beings they are used in. They are also more likely to have blood incompatibility in living beings. Such problems are more likely in allografts compared to xenografts.[26,27]

The use of autograft is the use of tissue taken from a different part of the body of the same living being in a different part of the body of the same person. They are considered the most effective among natural grafting methods due to their biocompatibility, non-toxicity, and minimal risk of immunological issues, such as allergic reactions. Autografts provide efficient integration with the tissue of the region where they are used due to the osteogenic cells and protein types they contain, thus supporting bone growth. Despite that, the most common problem with autografts is the low and limited availability of donors, and the procedure can result in trauma and scarring at the donor site.[28,29]

These limitations in natural bone grafts have paved the way for the development and use of synthetic bone grafts, which offer promising alternatives. Synthetic bone grafts can be tailored for specific applications and are widely researched for their potential. Synthetic bone grafts are used as bone implants and fillings for healing in cases where the bone is damaged. Metals, polymers and ceramics have been chosen as synthetic bone graft materials for such applications. One of the primary difficulty in creating synthetic bone grafts is to ensure biocompatibility with body tissue in terms of mechanics and structure. Therefore, metals and their alloys have been preferred in most applications due to their high mechanical properties. However, they

lack osteoconductivity (supporting bone growth), osteoinductivity (stimulating new bone formation), and osteointegration (forming a chemical bond with bone without a layer with fibrous membrane). In synthetic bone grafts used as bone filling materials, the choice of ceramic-based material stands out because it has properties similar to the bone structure. [30,31]

## **2.4. Synthetic Bone Grafts**

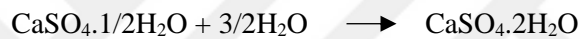
It is a medical necessity to prevent and fill the local bone losses caused by aging or trauma in the bone. There are many treatment techniques in these applications, and the surgeon must choose the most appropriate one according to the patient's condition. Each technique may have its own advantages and disadvantages. There are some limitations in bone amounts and morbidity when harvesting autogenous bone grafts. In addition, it is stated in medical reports that allografts, which are natural bone grafts, have a fracture incidence and cause postoperative infections that increase the risk of disease transmission. In the past quarter century, various synthetic grafts have entered our lives in order to reduce the above-mentioned and similar complications to the most optimum level. The most important features of synthetic bone grafts are that they are sterile, do not contain infections and viral diseases, and are easily accessible. [29]

Various materials have been used for many years to eliminate bone defects. These synthetic bone grafts have 2 of the features found in ideal bone substitute materials (Osteointegration, osteoconduction). Synthetic bone grafts should be similar to natural bone in terms of mechanics and biocompatibility. Apart from their biological compatibility, they should show fibrotic reaction and support bone formation by undergoing remodeling. In terms of mechanics, they should have a durability similar to the cancellous bone they replace as a substitute. They should have sufficient durability and elastic modulus under cyclic and routine loading. This is important to prevent fatigue fracture and stress shielding. Materials with these features are

calcium, aluminum or silicon based. [29]

#### 2.4.1. Calcium Sulfates

Calcium sulfates were used by Dreesman in the late 1800s. This work, which was done to fill bone defects and gaps in the bone, is considered the pioneering work of synthetic bone grafts used as bone defect fillers. During the 1950s and 1960s, Peltier expanded the clinical applications of calcium sulfates. [32] The exothermic reaction of calcium sulfate hemihydrate with an aqueous solution results in the formation of calcium sulfate dihydrate. The reaction is shown below. Calcium sulfates are generally used in the form of cement.



CSD, which has a large surface area and a porous structure resulting from the reaction, is a material with needle-like crystals. This porous structure facilitates the formation of new bone tissue. However, CSD has a high resorption rate, meaning it is broken down faster than new bone tissue can form, which is not ideal for bone defect reconstruction. In order to solve the problem of high resorption rate, calcium sulfate cements are used together with other bone graft materials. In this way, the resorption rate reaches more acceptable levels. [33,34].

## 2.4.2. Calcium Phosphate Ceramics

Calcium phosphates (CaP) are highly promising as bone substitute materials due to their chemical and structural resemblance to the mineral component of natural bone. Approximately 1 century ago, calcium phosphate ceramics began to be used in medical applications as bone repair materials due to their biocompatibility and bioactive properties.[35] In the 1920s, Tricalcium phosphate was first used as a bone substitute with in vivo implantation. The pioneers of this work were Albee and Morrison.[36] With the development of technology, the studies accelerated and in the mid-1900s, Ray used hydroxyapatite instead of implantation in guinea pigs.[37] After these pioneering studies, various calcium phosphate compounds were synthesized in accordance with biological standards and began to be used in biomedical applications.[38] Table 2.1 offers an overview of different CaP compounds, detailing their Ca/P molar ratios and additional characteristics.

Table 2.1 Calcium phosphate varieties with solubility, Ca/P molar ratio and pH stability properties [35]

Ca/P molar ratio	Compound	Formula	Solubility at 25°C, g/L	pH stability range in aqueous solutions at 25°C
0.5	Monocalcium phosphate monohydrate (MCPM)	$\text{Ca}(\text{H}_2\text{PO}_4)_2 \cdot \text{H}_2\text{O}$	~18	0.0-2.0
0.5	Monocalcium phosphate anhydrous (MCPA or MCP)	$\text{Ca}(\text{H}_2\text{PO}_4)_2$	~17	Stable at temperatures above 100°C
1.0	Dicalcium phosphate dihydrate (DCPD), mineral brushite	$\text{CaHPO}_4 \cdot 2\text{H}_2\text{O}$	-0.088	2.0-6.0
1.0	Dicalcium phosphate anhydrous (DCPA or DCP), mineral monetite	$\text{CaHPO}_4$	-0.048	Stable at temperatures above 100°C
1.33	Octacalcium phosphate (OCP)	$\text{Ca}_8(\text{HPO}_4)_2(\text{PO}_4)_4 \cdot 5\text{H}_2\text{O}$	-0.0081	5.5-7.0
1.5	$\alpha$ -Tricalcium phosphate ( $\alpha$ -TCP)	$\alpha\text{-Ca}_3(\text{PO}_4)_2$	-0.0025	Not possible to precipitate from aqueous solutions
1.5	$\beta$ -Tricalcium phosphate ( $\beta$ -TCP)	$\beta\text{-Ca}_3(\text{PO}_4)_2$	-0.0005	Not possible to precipitate from aqueous solutions
1.2-2.2	Amorphous calcium phosphate (ACP)	$\text{Ca}_x\text{H}_y(\text{PO}_4)_z \cdot n\text{H}_2\text{O}$ , n=3-4.5; 15-20% $\text{H}_2\text{O}$	Not measured precisely	~5-12 (always metastable)
1.5-1.67	Calcium-deficient hydroxyapatite (CDHAp or CDHA)	$\text{Ca}_{10-x}(\text{HPO}_4)_x(\text{PO}_4)_{6-x}(\text{OH})_{2-x}$ (0<x<1)	-0.0094	6.5-9.5
1.67	Hydroxyapatite (HAp or HA or OHAp)	$\text{Ca}_{10}(\text{PO}_4)_6(\text{OH})_2$	-0.0003	9.5-12
1.67	Fluorapatite (FA or FAp)	$\text{Ca}_{10}(\text{PO}_4)_6\text{F}_2$	-0.0002	7-12
2.0	Tetracalcium phosphate (TTCP or TetCP), mineral hilgenstockite	$\text{Ca}_4(\text{PO}_4)_2\text{O}$	-0.0007	Not possible to precipitate from aqueous solutions

The solubility of calcium phosphate compounds in aqueous environments is very important in terms of their areas of use. Because their solubility also affects their degradation rate. For example, if any CaP compound is less soluble than the compound found in the mineral part of the bone, its degradation will also occur very slowly. Conversely, if a CaP compound is more soluble than the bone mineral, it will degrade more quickly. For specific applications, it's important to choose a CaP compound with the appropriate solubility.[38] For instance, if the goal is to support Figure 2.3 shows the water solubilities of different CaP compounds. If the calcium phosphate to be selected from this figure is expected to form new bone, it must be one biodegradable in the body.

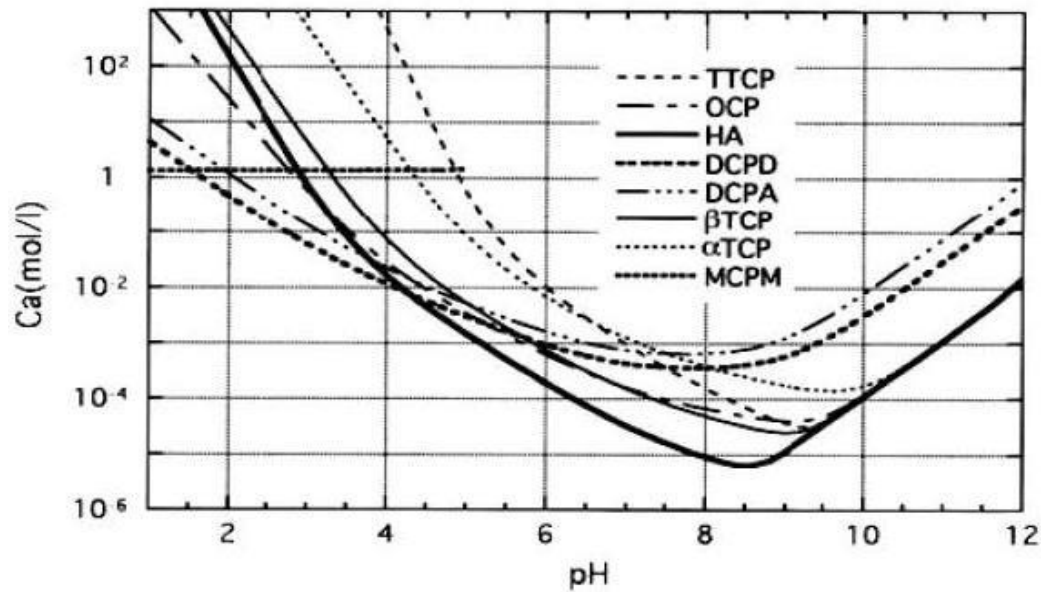


Figure 2.3. Solubility isotherms for various calcium phosphate compounds in aqueous media, depending on pH levels [36]

The solubility data for various calcium phosphate (CaP) compounds, as illustrated in Figure 2.3, influences their performance *in vivo*, while their pH stability provides insights into the long-term viability of CaP implants. Typically, CaP compounds with a Ca/P ratio between 1 and 1.67 are preferred for biomedical applications. Compounds with a Ca/P ratio below 1, such as MCPM and MCPA, exhibit higher acidity and solubility, making them less suitable for implantation. Conversely, those with a Ca/P ratio above 1.67, such as TTCP, demonstrate higher basicity and are also unsuitable for direct use in the body.[37] To solve the problems described, efficient CaP materials are mixed with less suitable CaP materials and put into service. As shown in Table 2.1, the most suitable calcium phosphate types for use in medical applications are Hydroxyapatite and tricalcium phosphate compounds.

### 2.4.3. Hydroxyapatite

As a result of the studies, research and product developments made by scientists named Aoki, Jarcho and de Groot in the last quarter of the 1900s, Hydroxyapatite began to be commercialized in medical applications.[38,39,40]

Since not all bone damage is the same, hydroxyapatite has been used in different forms such as block, granule and powder for bone regeneration. Since its mechanical properties are low when used alone, it is used in composite form with ceramics and polymers in applications requiring mechanical strength. Stoichiometric highly crystalline hydroxyapatite, with the formula  $\text{Ca}_{10}(\text{PO}_4)_6(\text{OH})_2$ , offering superior biocompatibility and stability in aqueous solutions compared to other calcium phosphate compounds, as illustrated in Figure 2.3. Pure HAp crystallizes in the monoclinic space group but transforms to a hexagonal phase at temperatures above 250 °C. Impurities can stabilize the hexagonal form at room temperature, so natural HAp typically exhibits this hexagonal structure.[41,42,43]

There are many different methods for HAp synthesis. The most efficient ones in terms of final product quality and quantity are solid-state reactions and wet synthesis methods. In the most preferred solid-state reactions, calcium phosphate precursors are baked in ovens above 1200 °C to obtain a homogeneous and crystalline HAp final product. However, this method produces crystals that differ in size and shape from those in natural bone. Wet methods for HAp preparation include precipitation, hydrothermal processes, sol-gel techniques, and hydrolysis of other calcium phosphates. These methods generally yield poorly crystalline and non-stoichiometric forms of HAp, often resembling calcium-deficient hydroxyapatite (CDHAp).[44,45,46]

#### 2.4.4. Calcium Deficient Hydroxyapatite

Calcium deficient HA is chemically and structurally similar to human bone structure and teeth. Calcium deficient HA has a Ca/P ratio of 1.5-1.67 and is represented by the formula  $\text{Ca}_{(10-x)}(\text{HPO}_4)(\text{PO}_4)_{(6-x)}(\text{OH})_{(2-x)}$ . ( $0 < x < 1$ ). It can be produced by solid-state reactions as well as by wet synthesis of calcium phosphate compounds at controlled pH and temperatures. [47,48,49]

CDHAp nanocrystals share similar physicochemical properties with bone mineral structures. [50] HA is a promising material for the use of calcium deficient bone grafts. Its prominent features are the high solubility of its nanocrystals and the high resorption rate. [51,52]

#### 2.4.5. Tricalcium Phosphate

The material called TCP can be found in powder, granule or as a whole block. TCP, a physiological mineral salt, shows three different polymorph forms. These are  $\beta$ -TCP,  $\alpha$ -TCP and  $\alpha'$ -TCP. Since  $\alpha'$ -TCP transforms into  $\alpha$ -TCP at transition temperatures, its use is limited and impractical [54]. While  $\alpha$ -TCP can be used stably at room temperature with effective and rapid cooling methods, the  $\beta$ -TCP polymorph shows a stable behavior at room temperatures. At 1125 °C,  $\beta$ -TCP transforms into  $\alpha$ -TCP form. The densities and solubilities of these two polymorphs are different and both are used in the orthopedics and dentistry industries for various purposes.[53,55,61]

#### 2.4.6. $\beta$ - Tricalcium Phosphate

$\beta$ -tricalcium phosphate, which has osteoconductive and osteoinductive properties, is among the most preferred synthetic bone grafts for use in the regeneration of bone defects.  $\beta$ -TCP, which also stands out with its biocompatibility, is in a stable phase at room temperature.[56]

As shown in Figure 2.3, hydroxyapatite has the most stable structure in an aqueous environment and is more preferred in implants that are used for long-term use.

$\beta$ -TCP, on the other hand, is less stable and degradable than hydroxyapatite. Thus, it can be used in new bone formations. When used in these applications, pore sizes are carefully examined.[57]

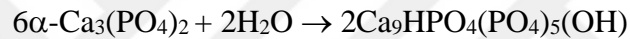
$\beta$ -TCP can be used as a two-phase bioceramics or composite by combining with different calcium phosphates. It is obtained by thermal decomposition at temperatures above 800 °C. [58,59]

#### 2.4.7. $\alpha$ - Tricalcium Phosphate

There are various synthesis methods to produce pure  $\alpha$ -TCP.  $\alpha$ -TCP shows a stable structure at high temperatures, but at low temperatures such as room temperature, its stable structure deteriorates and it shows a metastable behavior. Thermal conversion of a calcium phosphate compound with a Ca/P ratio of 1.5 can be used to produce pure  $\alpha$ -TCP. For instance, a CDHAp precursor, created by precipitating calcium and phosphate with a Ca/P ratio of 1.5, can be converted to  $\alpha$ -TCP by heating at 1250 °C for 2 hours. Alternatively,  $\alpha$ -TCP can be synthesized produced from amorphous calcium phosphate under lower temperature conditions, between 600 and 800 °C. The most straightforward method involves heating  $\beta$ -TCP to its transformation temperature of approximately 1125 °C and then applying effective quenching.[57,60]

Solid state reactions are a different technique used for  $\alpha$ -TCP production.  $\alpha$ -TCP synthesis is achieved by solid state reaction of calcium and phosphate precursors such as  $\text{CaCO}_3:\text{NH}_4\text{H}_2\text{PO}_4$ . In order to mix the precursors better, they are milled and baked in ovens at a certain temperature (1200 to 1500 °C) for 2-48 hours. In order to avoid the formation of other phases ( $\beta$ -TCP), sudden cooling processes are applied and pure  $\alpha$ -TCP synthesis is achieved.[62]

Despite having the same chemical composition,  $\alpha$ -TCP and  $\beta$ -TCP differ significantly in solubility.  $\alpha$ -TCP is more soluble than  $\beta$ -TCP, which makes it a key component in apatitic calcium phosphate cement.  $\alpha$ -TCP reacts with water to convert into hydroxyapatite (HAp), as described in Equation 2. This reaction results in a hardened solid mass in the form of cement. [60,62]



Among the various calcium phosphates,  $\alpha$ -tricalcium phosphate ( $\alpha$ -TCP,  $\text{Ca}_3(\text{PO}_4)_2$ ) stands out due to its numerous beneficial characteristics, including its high solubility in aqueous environments, its ability to undergo a hydration reaction at physiological pH, and the subsequent formation of calcium-deficient hydroxyapatite (CDHA) upon setting. These factors contribute to the material's notably bioresorbable nature.  $\alpha$ -TCP exhibits superior solubility in aqueous solutions compared to the  $\beta$ -phase, which enhances its reactivity and resorbability, ultimately enabling its hydration into CDHA. This form of hydroxyapatite is chemically, crystallographically, and morphologically closer to the bone mineral phase. The fabrication of  $\alpha$ -TCP-based cements is notably intricate, as several factors influence the properties of calcium phosphate cements (CPCs), such as the particle size, solid to liquid (s:l) ratio, and the proportion of the amorphous phase.[63]

The compressive strength of the cement is closely linked to the degree of hydration of  $\alpha$ -TCP and the subsequent precipitation of CDHA crystals. During the hydration of  $\alpha$ -TCP, CDHA crystals precipitate on the surface of the cement, and the formation of an interlocking crystal network contributes to the cement's hardening behavior.

The strength of the cement is influenced by the morphology, size, arrangement, and packing density of these crystals. As the crystals grow, it is anticipated that the number of contact points will increase, leading to the development of a network capable of withstanding mechanical stress. The mechanical properties evolve over the course of the setting reaction: initially, the cement contains minimal precipitated CDHA and exhibits low compressive strength; however, as the reaction progresses, the formation of precipitates and the interlocking of crystals result in an increase in mechanical strength.

## **2.5. Objective and general structure of the thesis**

The objective of this thesis is to produce  $\alpha$ -tricalcium phosphate ( $\alpha$ -TCP) with high purity through reactive solid-state synthesis and subsequently investigate its hydration behavior under various conditions. The main focus is to examine the hydration behavior (cement-type conversion upon water uptake) of the synthesized  $\alpha$ -TCP powders based on different physico/chemical parameters as schematically shown in Figure 2.4. The conversion is expected to form calcium-deficient hydroxyapatite (CDHAp), a bone mineral analog. Therefore, the extended scientific/technological value of the thesis is to explore the potential of use of  $\alpha$ -TCP for irregular hard tissue defect filling operations. The studies in the thesis however, only include very immature and early material-related aspects for developing a biomaterial.

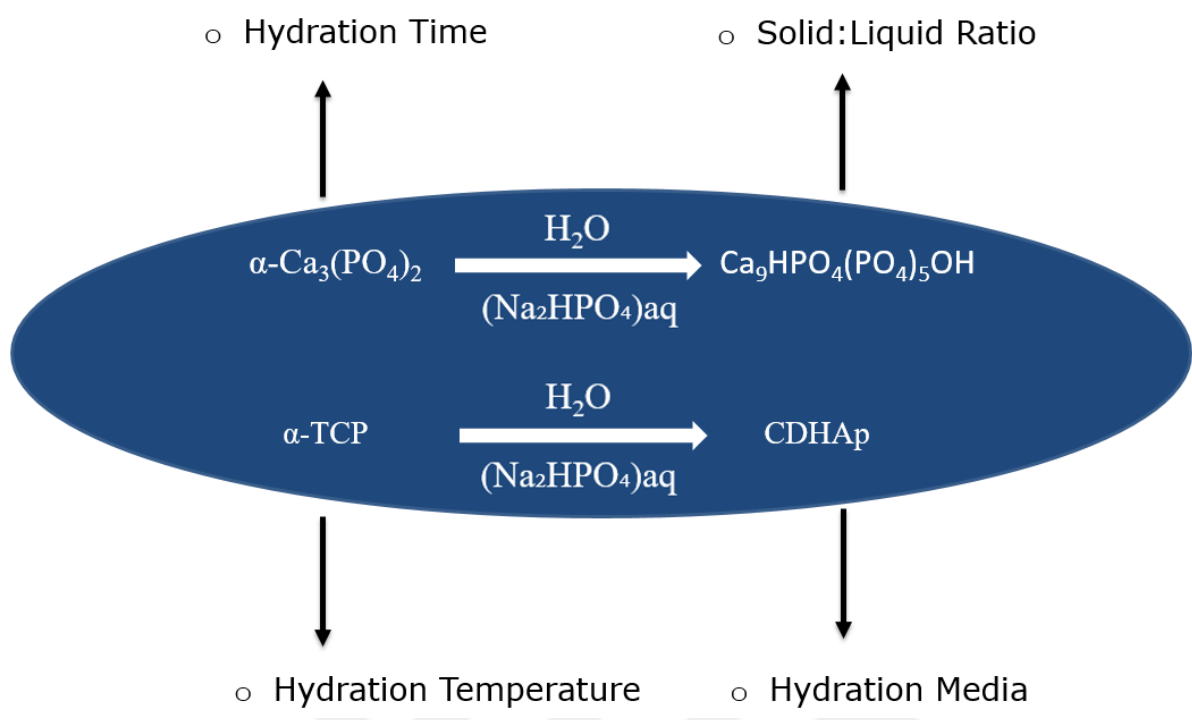


Figure 2.4. The rational planning and outline of the thesis

The parametric studies on hydration of  $\alpha$ -TCP involved; exploring the effect of solid-to-liquid ratio of the cement mixtures, hydration kinetics, the effect of hydration temperature and hydration media, with the goal of identifying the optimal hydration conditions.

The experimental studies and results/discussion are presented in two chapters. Chapter 3 outlines the materials used, methods and analytical characterization techniques employed in the thesis.

In Chapter 4, where the experimental results and finding are presented and discussed, formation of  $\alpha$ -TCP by a solid-state reaction between monetite and calcium carbonate precursors is introduced. In the rest of the all studies, this custom-synthesized reactant used. The resultant  $\alpha$ -TCP powders were hydrated with DI water and/or  $(\text{Na}_2\text{HPO}_4)_{\text{aq}}$  at different solid-to-liquid ratio, reaction temperatures

and different hydration times. All these parameters influencing their conversion to calcium-deficient hydroxyapatite (CDHAP) were thoroughly examined and evaluated. The characterization were conducted on both the  $\alpha$ -TCP and the products obtained after hydration, and results were interpreted/explained in terms of phase evolution/identification, morphological characteristics and mechanical properties.





## CHAPTER 3

### MATERIALS AND METHODS

The  $\alpha$ -tricalcium phosphate ( $\alpha$ -Ca<sub>3</sub>(PO<sub>4</sub>)<sub>2</sub> or  $\alpha$ -TCP) powders were produced through high-temperature solid-state reaction using custom-synthesized and/or readily available solid reactants. This part of the thesis details the experimental procedures for synthesis  $\alpha$ -TCP; methodology in evaluating its' cement-type hydration efficiency and kinetics in DI water or aqueous solution of Na<sub>2</sub>HPO<sub>4</sub>, in a comparative way. Additionally, this chapter explains the analytical material characterization techniques and analysis methods employed in the thesis.

$\alpha$ -TCP was used as the base material-main single cement reactant-and all physico-chemical analyses and were accomplished using this material. Starting materials and synthesis approach of  $\alpha$ -TCP plays an important role, in controlling the cement reactivity. As  $\alpha$ -TCP is not the thermodynamically room temperature stable TCP polymorph, it can be only obtained by following a solid-state reaction and following a non-equilibrium conditions during high temperature chemical formation. Therefore,  $\alpha$ -TCP was custom-synthesized according to an original recipe using simple Ca- and P-precursors. The experimental details regarding the synthesis of  $\alpha$ -TCP; and the formation of a low temperature (at around physiological temperature) hardened hydroxyapatite resulting from cement-type hydration of  $\alpha$ -TCP are presented. Following the synthesis information, in parallel to the objectives of the thesis, the experimental method details of the parametric studies, on exploring the kinetics of cement-type hydration of  $\alpha$ -TCP, the effect hydration temperature, solid to liquid ratio, hydration time and hydration media (DI vs. common ion containing aqueous solutions) are also presented in this chapter.

### 3.1. Materials

$\alpha$ -TCP was synthesized according to the chemical/physical preparation flow chart, as outlined in Figure 3.1. The flowchart also shows the chemical transformation, decomposition reactions for obtaining intermediate calcium phosphate (CaPs) compounds during this synthesis protocol.

In simple words,  $\alpha$ -TCP powders were produced by the solid-state reaction of calculated amounts of calcium carbonate ( $\text{CaCO}_3$ , Merck, Germany) and laboratory synthesized monetite ( $\text{CaHPO}_4$ ) in an open air furnace at  $1200^\circ\text{C}$ . for 2 hours. Calcium carbonate and phosphoric acid ( $\text{H}_3\text{PO}_4$ , 85 wt%, Merck, Germany) were main as-received reagents

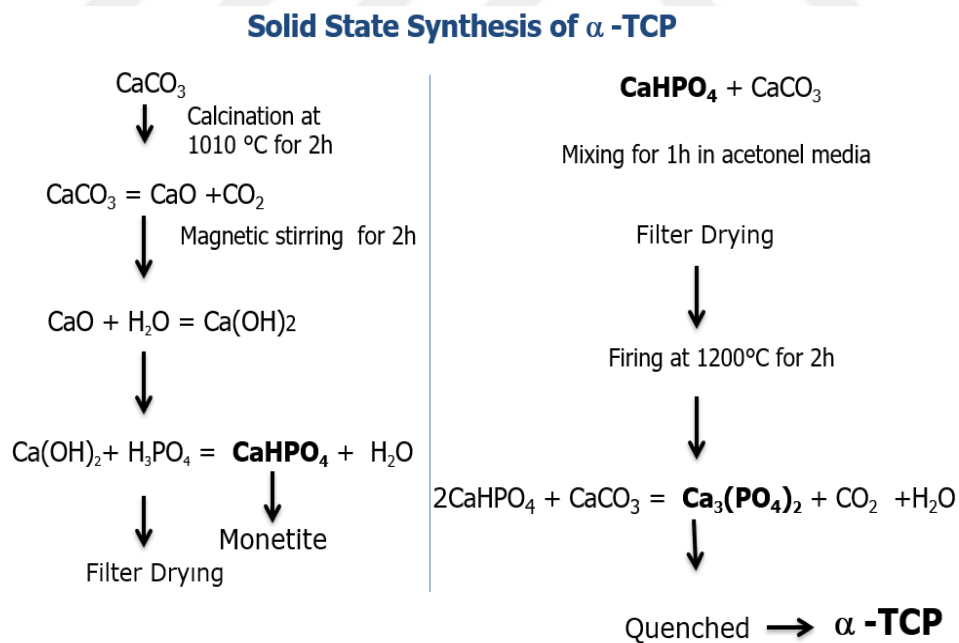


Figure 3.1. Synthesis details of  $\alpha$ -TCP including the chemical reactions leading to formation of intermediate reactants and final product  $\alpha$ -TCP.

used for synthesis.  $\text{CaCO}_3$  served as the calcium source,  $\text{H}_3\text{PO}_4$  was the phosphorus source for intermediate CaPs.  $\text{CaCO}_3$  and  $\text{CaHPO}_4$  (intermediate CaP phase) were mixed in stoichiometrically calculated proportions and fired high temperature to form TCP, where  $\alpha$ -TCP becomes thermodynamic the most stable polymorph among many polymorphs of TCP ( $\beta$ ,  $\gamma$  etc.).

## 3.2. Experimental Procedures

### 3.2.1. Preparation of Monetite ( $\text{CaHPO}_4$ ): Solid reactant for $\alpha$ -TCP

As shown on the left hand side of the flowchart in Figure 3.1,  $\text{CaHPO}_4$  is obtained from  $\text{CaCO}_3$ . First,  $\text{CaCO}_3$  was calcined, to obtain  $\text{CaO}$ , then after mixing with DI-water,  $\text{Ca}(\text{OH})_2$  was obtained, and this was followed by addition of phosphoric acid to incorporate  $\text{PO}_4$  groups to calcium hydroxide in order to precipitate as  $\text{CaHPO}_4$ . Calcination of  $\text{CaCO}_3$  to  $\text{CaO}$  was performed at  $1010^\circ\text{C}$  for 2 hours in open air furnace. After confirming the formation of phase pure  $\text{CaO}$  (by XRD),  $\text{CaO}$  powders were added into excess DI water and mixed by magnetic stirrer for 1 hour. Later on,  $(\text{H}_3\text{PO}_4)_{\text{aq}}$  is added drop-wise to the  $\text{Ca}(\text{OH})_2$  slurry with a molar ratio of 1:1 at  $60^\circ\text{C}$ , and after additional mixing for 1.5 hours reaction, the slurry was vacuum filtered. The product was dried in an oven at  $70^\circ\text{C}$  for 2 days. The reaction products were then analyzed for phase characteristics by XRD.

### 3.2.2. Preparation of $\alpha$ -TCP

As shown in Figure 3.1 (right hand side of the flowchart)  $\alpha$ -TCP was obtained by mixing previously prepared  $\text{CaHPO}_4$  (according to 3.2.1) and starting  $\text{CaCO}_3$  powders in high density polyethylene cup (Nalgene<sup>TM</sup>) by using a Turbula mixer. After 1 hour mixing, powder mixture was filled into alumina crucible and fired at  $1200^\circ\text{C}$  in open atmosphere for 2 hours. After firing, an effective air quenching is applied on partially fused red-hot fired compacts, and quenched compacts were

downsized by using alumina mortar and pestle. By this way, a standard, large mother batch of  $\alpha$ -TCP (approx. about 150 gr) was obtained, and same batch had been used throughout the all studies in the thesis without any further physical modification/treatment on this batch, without changing particle properties. This batch was sealed and stored in a desicator in long-time use/studies.

### 3.3. Evaluation of hydration behaviour of $\alpha$ -TCP

The cement type reactivity  $\alpha$ -TCP, i.e., hydration efficiency towards forming calcium-deficient hydroxyapatite (CDHAp,  $\text{Ca}_{10-x}(\text{HPO}_4)_x(\text{PO}_4)_{2-x}(\text{OH})_{2-x}$ ) by water uptake was examined a simple approach. After initiating hydration by mixing free  $\alpha$ -TCP powders (pre-determined amount) with DI water (pre-determined amount), hydration was conducted in DI-water filled sealed plastic containers, submerged in a water bath constant temperature.

During these studies, the effects of various reaction parameters, **(i)** hydration temperature, **(ii)** solid-to-liquid ratio ( $\alpha$ -TCP powder: DI-water weight ratio), **(iii)** hydration time on CDHAp formation efficiency had been examined. Initially,  $\alpha$ -TCP powders were mixed with DI-H<sub>2</sub>O at solid-to-liquid weight ratios of 1:1, 1:3, and 1:5. Subsequently, conversion to CDHAp was performed, by resting cement mixtures ( $\alpha$ -TCP+H<sub>2</sub>O) in a water bath for 1, 12, and 24 hours at of 25 °C, 37 °C, and 60 °C. The conversion to cement product CDHAp, was monitored through phase analyses using x-ray diffraction (XRD), as well by microstructural analyses using scanning electron microscopy (SEM) analysis.

In addition to these parametric studies, another one, **(iv)** the effect of a common-ion containing hydration media, instead of DI-water, on cement type reactivity of  $\alpha$ -TCP has been separately investigated. For this purpose, first  $\alpha$ -TCP powders were mixed

with aqueous  $\text{Na}_2\text{HPO}_4$  (Merck, Germany) instead of pure DI-water at solid-to-liquid weight ratios of 1:3. Three different  $\text{Na}_2\text{HPO}_4$  solutions with varying ionic strength, with nominal compositions of 1 wt.%, 2.5 wt. and 5 wt%, rest being DI-water were used as hydration media. Subsequently,  $\alpha\text{-TCP} \rightarrow \text{CDHAp}$  was achieved by maintaining these cement mixtures in a water bath for 1, 5, 12, and 24 hours at 37 °C. Again, final products were analyzed using XRD and SEM.

#### **3.4. Preparation of samples for mechanical evaluation of the cement reaction:**

For mechanical testing customized pellets were formed in parallel to powder-based cement-type hydration kinetic studies. First,  $\alpha\text{-TCP}$  powders were consolidated into 15 mm thick coin-like circular pellets of 3 mm in diameter. For this purpose, 1.5 g of TCP powder were pressed (Model-C, Carver Inc., IN, USA) uniaxially in a cylindrical die at a pressure of 4 MPa at ambient temperature.

The shaped  $\alpha\text{-TCP}$  pellets were simply reacted with DI-water or  $\text{Na}_2\text{HPO}_4$  in order to start cement reaction and while keeping their proper geometry in hydration media, which required for testing/measurement. The  $\alpha\text{-TCP}$  pellets were typically inserted into plastic vials containing with DI-water (or  $\text{Na}_2\text{HPO}_4$  solution), and aqueous media amount was varied adjusted to selected solid to liquid ratios, based on the findings of powder-based cement-type hydration kinetic studies. In mechanical testing studies, final samples are produced only hydrating at 37 °C for 24 hours- with the help of constant temperature water bath. Some pressed pellets were kept in as-pressed condition as reference samples.

### **3.5. Phase identification: X-Ray Diffraction Analysis:**

Phase identifications by x-ray diffraction (XRD) performed during  $\alpha$ -TCP synthesis to evaluate the characteristics of the intermediate/final compounds formed during synthesis of  $\alpha$ -TCP, as well as to evaluate kinetics/products of cement-type hydration reaction.  $\text{CuK}\alpha$  radiation was employed with an operating voltage of 40 kV and a current of 30 mA. The calcium phosphate powders and cement end products were scanned in the  $2\theta$  range of  $20^\circ$ - $40^\circ$ .

### **3.6. Microstructural investigation: Scanning Electron Microscopy**

The microstructure of the powders, pre-cement hybrid mixtures, was examined using a FEI Quanta 400F field emission scanning electron microscope (SEM). The samples were gold-coated prior to the SEM analysis.

### **3.7. Mechanical Testing: Diametral Compression Test**

The mechanical property, fracture strength, of cement products (derived from hydration of  $\alpha$ -TCP with DI water or  $\text{Na}_2\text{HPO}_4$  solution) were determined using diametral compression test. The schematic in Figure 3.2 shows set-up for diametral compression, which is very practical assessment tool for brittle ceramic-like pellets, not exhibiting plastic deformation, with coin-like geometry.

The testing was conducted using a Shimadzu AGS-J 10 kN universal testing machine with a crosshead speed of 0.5 mm/min at room temperature. The fracture strength ( $\sigma$ , in MPa) of the pellets was determined using the following formula:

$$\sigma = 2P/\pi Dt$$

where:

- P is the maximum compressive load (in N) that the pellets can sustain before fracture,
- D is the diameter (in cm) of the pellet, and
- t is the thickness (in cm) of the sample.

Typically, multiple pellets were tested to ensure representative data for each set of samples.

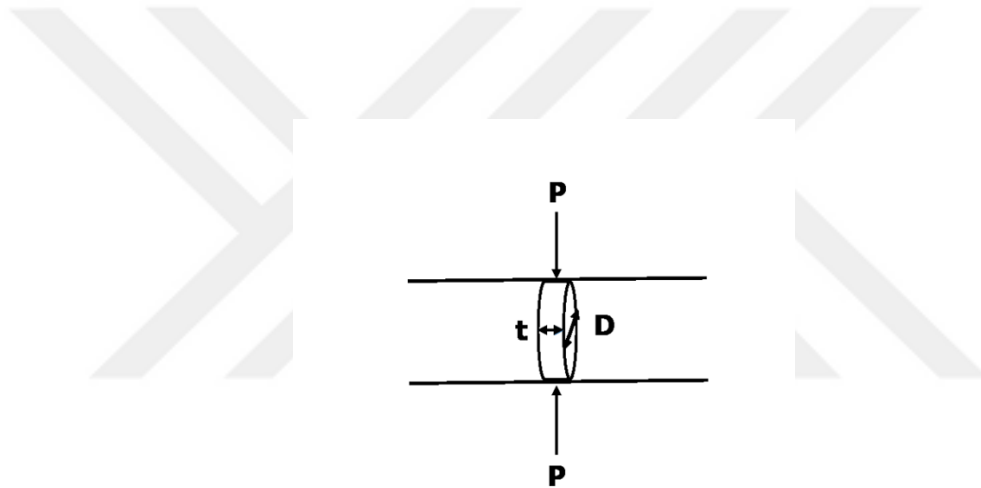


Figure 3.2 Schematic representation of diametral compression test



## CHAPTER 4

### RESULTS and DISCUSSIONS

This chapter presents the material synthesis results, i.e. the characterization of the solid-state reaction product, obtained through the preparation method detailed in the experimental chapter. X-ray diffraction (XRD) was used to analyze the phases to confirm the phase characteristics of the synthesized  $\alpha$ -TCP and also during hydration studies to investigate the cement product(s). The microstructural properties of these before mentioned systems were also assessed using scanning electron microscopy (SEM).

#### 4.1 Characterization of Monetite Powders

Figure 4.1. shows the XRD pattern of the powder form monetite, ( $\text{CaHPO}_4$ -one of the solid reactants needed for  $\alpha$ -TCP preparation) produced according to the experimental procedure explain in Figure 3.1. All the diffraction peaks belong to monetite in accordance with to JCPDS card no: 71-1759; assigned for monetite No other by-product/intermediate calcium phosphate phase was observed. This finding indicates a phase pure monetite, was obtained by wet chemical synthesis route.

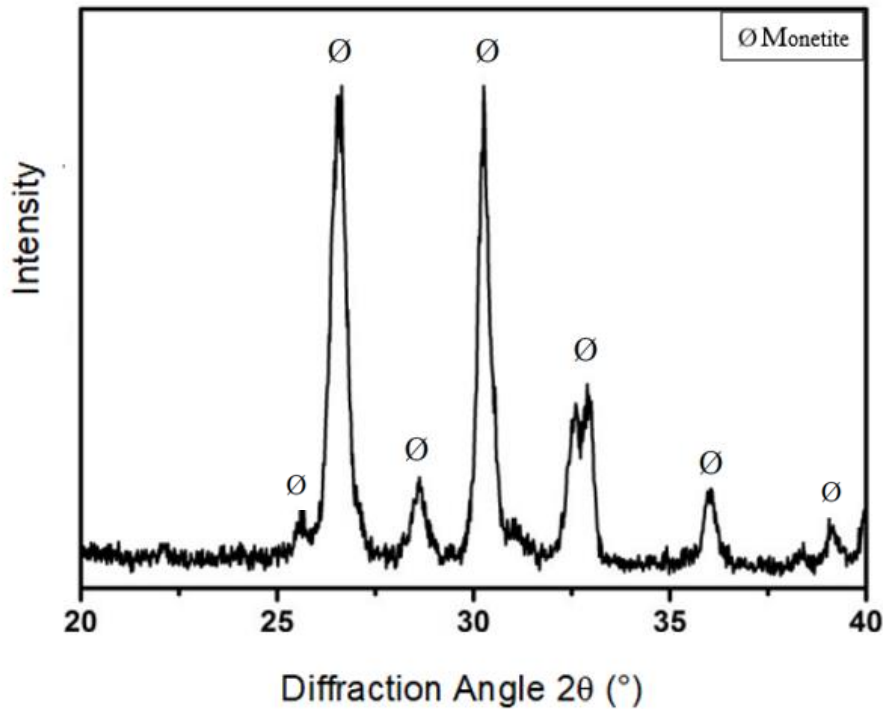


Figure 4.1. XRD Diffractogram for the product of Monetite

## 4.2 Characterization of $\alpha$ -TCP Powders

### 4.2.1 XRD Characterization of $\alpha$ -TCP Powders

The diffractogram presented in Figure 4.2 illustrates the XRD pattern of the powder sample produced through a solid-state reaction between calcium carbonate ( $\text{CaCO}_3$ ) and monetite ( $\text{CaHPO}_4$ ) mixture at  $1200\text{ }^\circ\text{C}$  (in air), followed by rapid cooling in air. The XRD pattern aligns perfectly with JCPDS card no 9-348 for  $\alpha$ -TCP. As no additional diffraction peaks corresponding to other crystalline phases or calcium phosphate compounds are observed, it can be concluded that the reaction product is phase-pure  $\alpha$ -TCP in its as-synthesized state. This data also indicate that the

formation of  $\beta$ -TCP was fully inhibited. This non-equilibrium TCP polymorph formation was achieved, implying that an efficient and successful quenching process was carried out. The phase-pure nature of  $\alpha$ -TCP synthesis product is also important for the cement-type conversion, because the  $\beta$ -polymorph does not hydrates and sets in to a hard product like the  $\alpha$ -polymorph.

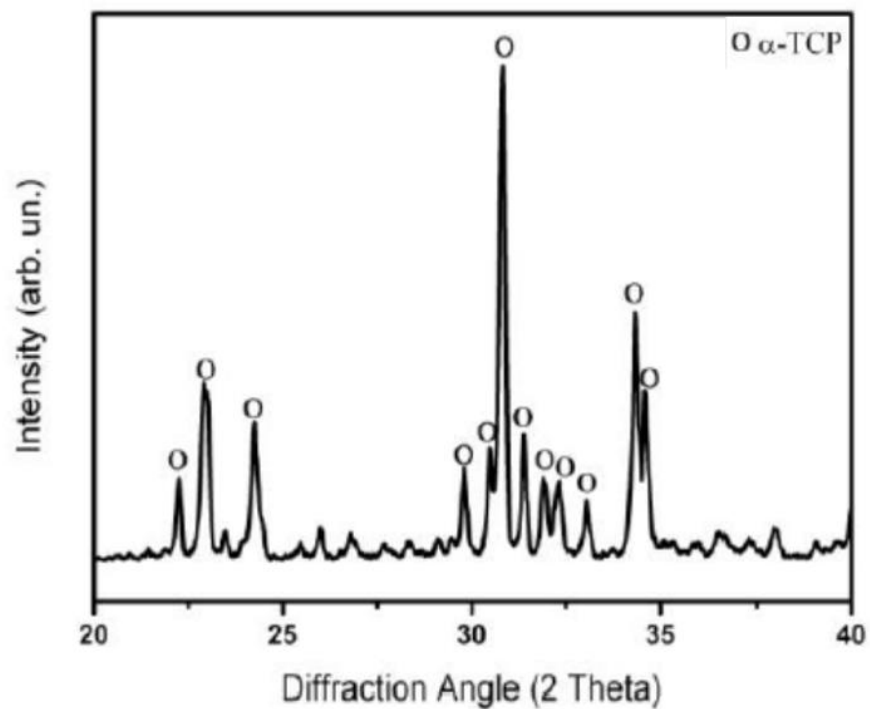


Figure 4.2. XRD diffractogram of  $\alpha$ -TCP powder

#### 4.2.2 SEM Characterization of $\alpha$ -TCP Powders

The SEM image in Figure 4.3 displays the typical microstructural features of the as-synthesized TCP (from mother batch). The irregular shapes of primary particles, exhibiting a smooth surfaces and sometimes fused-like morphology, are typical and in agreement with those observed in solid-state synthesized ceramic powders, as reported in previous studies [64] Based on the general view SEM images (not shown)

obtained at lower magnification, the typical average particle size for  $\alpha$ -TCP product is approximately  $6 \pm 2 \mu\text{m}$ .

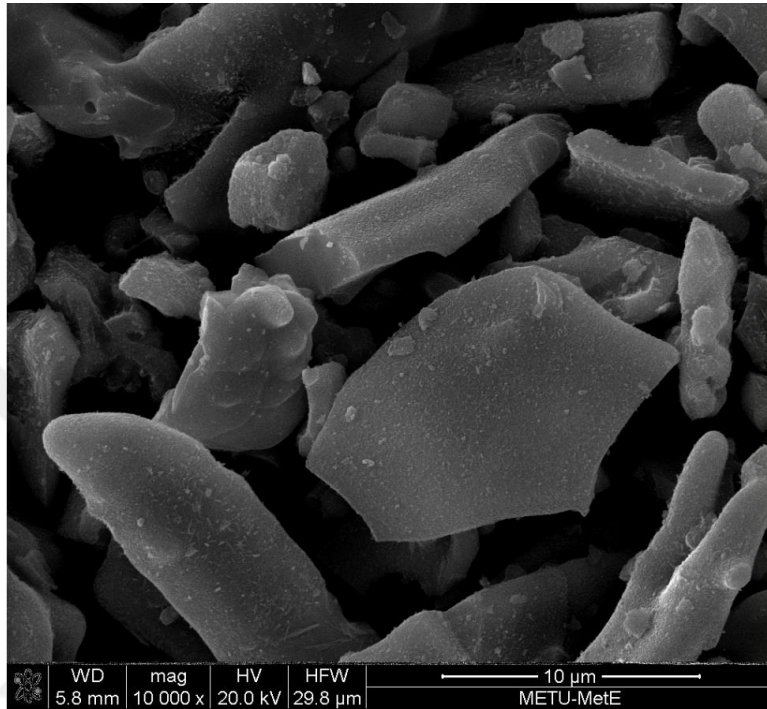


Figure 4.3. SEM micrograph of  $\alpha$ -TCP

### 4.3 Evaluation of hydration behavior of $\alpha$ -TCP: Effect of solid:liquid ratio

The diffractogram presented in Figure 4.4 illustrates the XRD pattern of the powder sample produced through a hydration of  $\alpha$ -TCP powders directly with DI water. Hydration of  $\alpha$ -TCP powders was carried out in a water bath at 37 degrees for 24 hours. The solid to liquid ratios of  $\alpha$ -TCP powders hydrated with DI water were adjusted to 1:1, 1:3 and 1:5. In other words, this set samples indicative for the first parameter, *solid:liquid ratio*, that may affect  $\alpha$ -TCP  $\rightarrow$  HAp conversion. The effects of the solid-to-liquid ratio can be analyzed by examining the peaks present in Figure 4.4.

The XRD data indicates that, in the case of the cement mixture with 1:1 solid:liquid ratio, the hydration does not proceed effectively, and complete conversion to HAp is hampered. (the pattern located at the bottom). This graph still exhibits the characteristic peaks, especially the most intense peak at around diffraction angle  $31^\circ$ , of the alpha-tricalcium phosphate ( $\alpha$ -TCP) reactant. However, it can be said that the conversion to hydroxyapatite (HAp) has commenced partially, indicated by three peaks in the  $2\theta$  range of  $31.5$ - $32.5$ , which all belong to HAp. It is worth to mention that XRD will not directly tell calcium-deficiency, but one can tell during conversion Ca/P ratio should be preserved. The Ca/P for  $\alpha$ -TCP [ $\text{Ca}_3(\text{PO}_4)_2$ ] is 1.50, and also 1.50 for [ $\text{Ca}_9(\text{HPO}_4)(\text{PO}_4)_5(\text{OH})$ ], which is fully calcium-deficient HAp. This would be 1.67 in the case of stoichiometric HAp with chemical formula [ $\text{Ca}_{10}(\text{PO}_4)_6(\text{OH})_2$ ].

In the case higher amount of hydration media (water) presence, i.e. for the cement mixture composed of  $\alpha$ -TCP and deionized (DI) water in a 1:3 ratio, the hydration efficiency changes significantly. As shown-by pattern in the middle, complete conversion to HAp is attained after 24 hours (maybe earlier). The characteristic peaks of  $\alpha$ -TCP are all absent, which can be clearly monitored by the missing strongest peak at around at around diffraction angle  $31^\circ$ , instead the diffraction peaks indicate a single-phase pure HAp. Same observation also holds for highest amount of water-involving cement mixture a solid:liquid ratio of 1:5. The top pattern of Figure 4.4. also indicates complete hydration of TCP to phase pure HAp. There is again no detectable peaks corresponding to  $\alpha$ -TCP. In conclusion, there synergistic effect of hydration media amount, which enables complete and most likely faster cement conversion in high amounts.

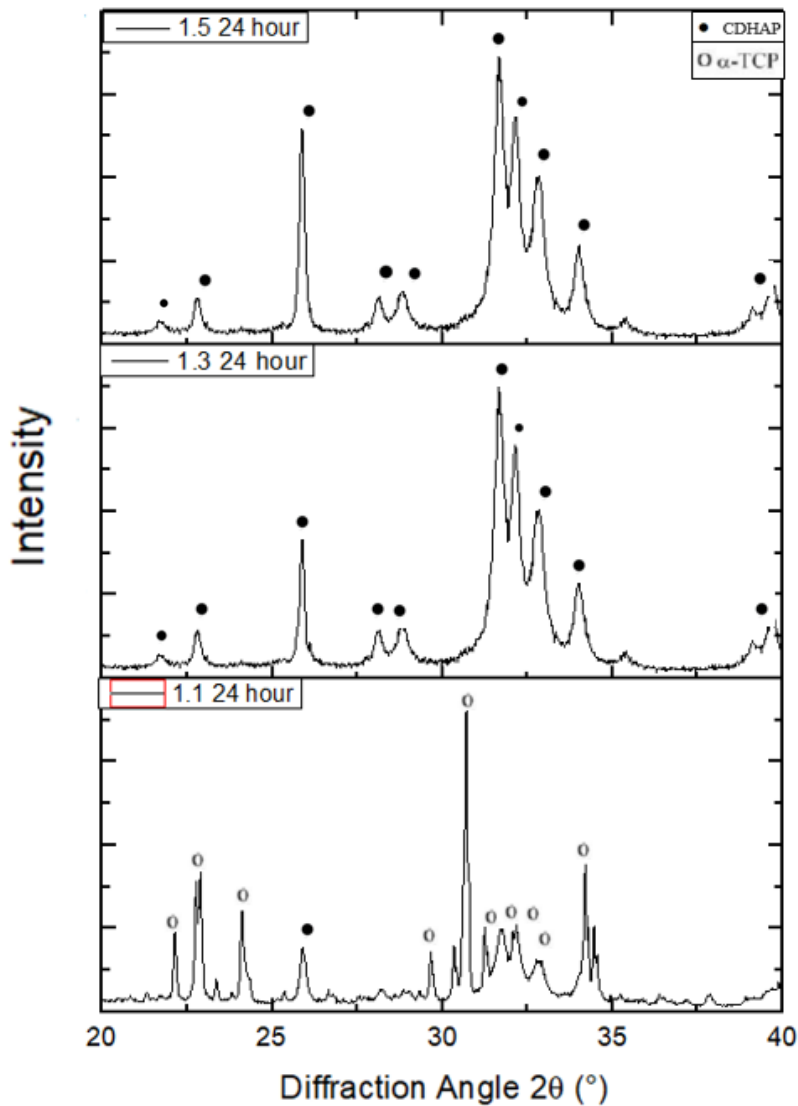


Figure 4.4. XRD diffractograms of  $\alpha$ -TCP powder, hydrated at different solid to liquid ratio (1:1, 1:3, 1:5) for 24 hours.

The microstructural changes upon hydration with different solid:liquid ratio of cement mixture have been also studied with help of SEM.

The top SEM image in Figure 4.5, is for the hydration product of the  $\alpha$ -TCP and DI water mixture in a 1:1 ratio for 24 hours at 37°C. The final product closely resembles

the typical SEM features of initial  $\alpha$ -TCP particles almost smooth surfaces. However, there very small white crystals on some TCP particles (for particles upper right corner), indicating formation of some CDHAp on the surfaces. These observations are consistent with the results shown in the XRD diffractogram presented in Figure 4.4; limited conversion to cement product.

The other two SEM images presented in Figure 4.5 provide insights into the morphology of the CDHAp products and the nature of hardening/setting achieved through hydration. The SEM images obtained for hydration studies of  $\alpha$ -TCP and DI water mixture in a 1:3 ratio for 24 hours at 37°C (micrograph in the middle) is distinctly different with flake/plate-like reticulated crystals. This microstructure is characteristic to CDHAp, formed by cement reaction, indicating formation of a crystal product by dissolution and reprecipitation. The CDHAp crystals exhibit a flake-like morphology and form an interlocked reticulated structure, which is consistent with findings reported by others [65]. The SEM image images obtained from hydrating the  $\alpha$ -TCP and DI water mixture in a 1:5 ratio for 24 hours at 37 °C (micrograph at the bottom) showed similar features as 1:3 cement mixture. Again, a flake-like morphology and interlocked, reticulated crystals reveal complete conversion to CDHAp. By considering that the images are obtained at same magnification, it can be said that the CDHAp crystals formed at the highest solid:liquid ratio are little bigger than crystals formed with lower amount of water, i.e. 1:3 solid:liquid cement mixture. However, this difference is not that significant/distinct.

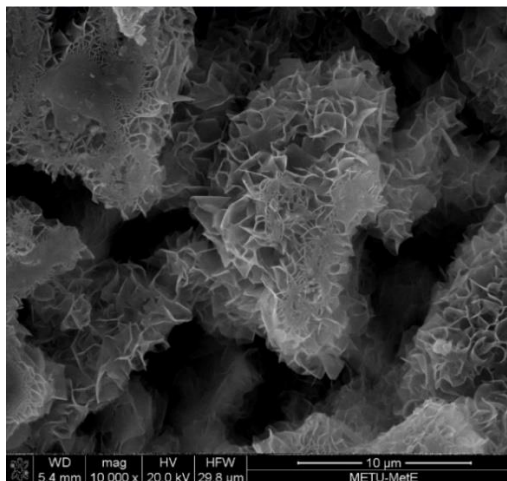
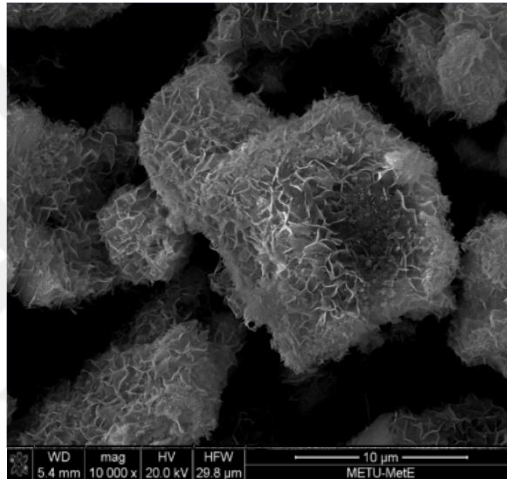
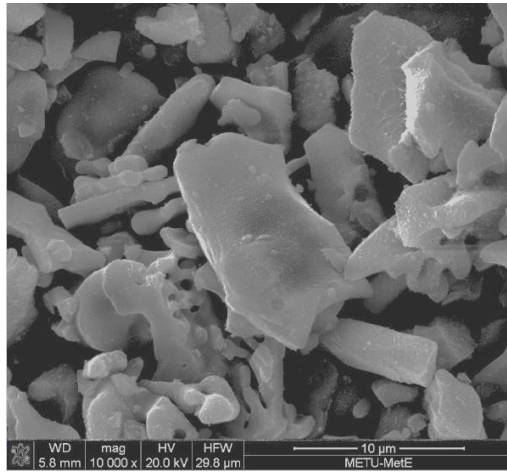


Figure 4.5 SEM micrographs of the product phase resulting from  $\alpha$ -TCP hydration for 24 hours, with a s:l ratio of 1:1, 1:3, 1:5, respectively (from top to bottom)

#### 4.4 Evaluation of hydration behavior of $\alpha$ -TCP: Hydration/reaction kinetics

In the second set experimental studies the effect of second hydration/reaction parameter, *reaction time/kinetics*, on  $\alpha$ -TCP  $\rightarrow$  HAp conversion has been examined. XRD and SEM were the two main analytical tools used for this purpose.

In order to investigate the effect of hydration time on cement conversion,  $\alpha$ -TCP powders were hydrated with DI water at 37 °C using a pre-determined solid-to-liquid ratio of 1:3, over various time intervals. The hydration was conducted uninterruptedly for 1, 4, 8, 12, 24, and 56 hours. The cement mixtures were maintained close vials in a water bath throughout these kinetic studies. The hydration has been stopped by washing and drying the samples with acetone to stop further hydration, at the end of hydration time of interest.

The XRD data for kinetics studies are presented in Figure 4.6, showing the phase characteristics of hydration product after selected times of hydration. Upon examining the hydration results at 1 hour and 4 hours in Figure 4.6, it is evident that CDHAp conversion has not occurred, and the characteristic XRD peaks of  $\alpha$ -TCP are still present. This lack of conversion may be attributed to the insufficient interaction time between the DI water and the  $\alpha$ -TCP powders, preventing initial dissolution of TCP required to achieve saturated condition for precipitation of hydrated product. The data for longer hydration times, i.e. for 8 and 12 hours revealed that the conversion to CDHAp has begun. However, since both the characteristic peaks of  $\alpha$ -TCP and CDHAp are still present, it can be inferred even 12 hours of hydration are not sufficient for complete transformation. Both for 24- and 56-hour hydrated samples on the other hand, the product is completely HAp, no diffraction peak of  $\alpha$ -TCP were observed for these samples. This suggests that both 24 and 56 hours of hydration are adequate for the complete conversion to CDHAp.

It can be concluded that, in the case of a solid:liquid ratio of 1:3, while DI-water being the hydration media at 37 °C,  $\alpha$ -TCP  $\rightarrow$  HAp conversion initiates somewhere in the time range of 4-8 hours, and completes somewhere 12-24 hours.

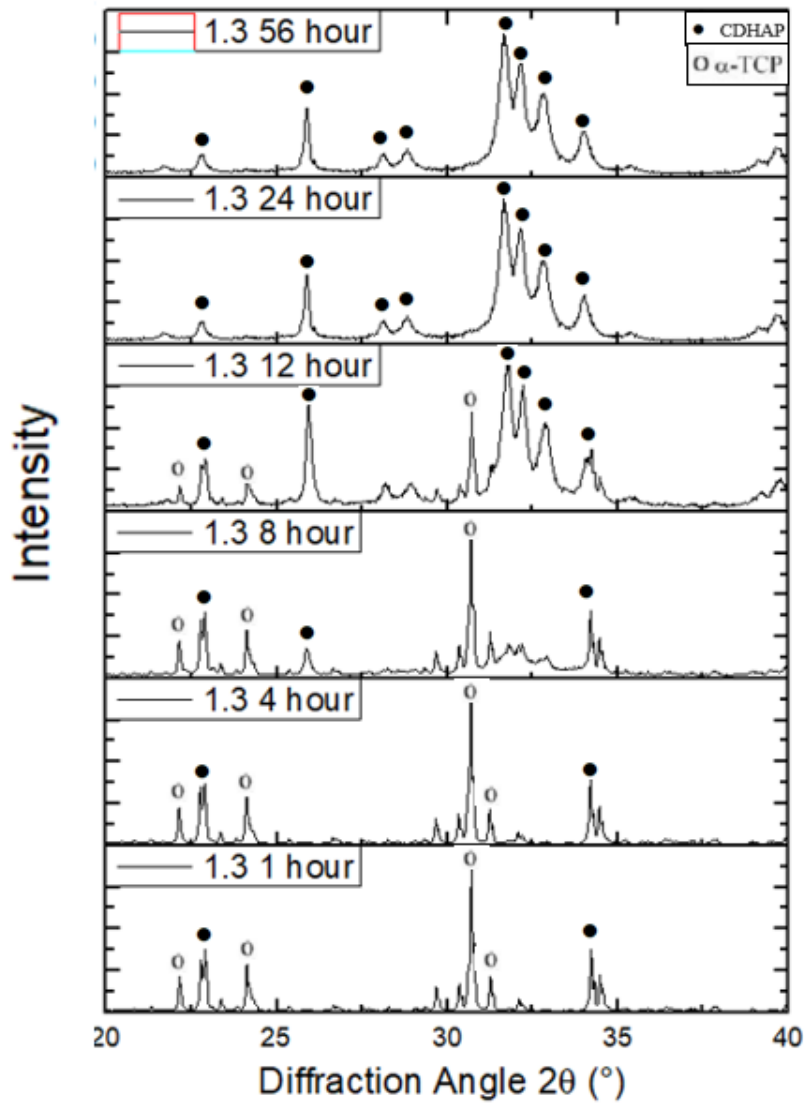


Figure 4.6. XRD diffractograms for the end product of hydration  $\alpha$ -TCP at 37°C with different reaction time. The solid:liquid ratio was of 1:3, and DI-water was the hydration media.

In addition microstructural investigation have been performed with to observe the effect of hydration time during cement conversion. The SEM images were obtained analyzed for  $\alpha$ -TCP samples hydrated 12, 24, and 56 hours. These specific hydration times were chosen based on the data obtained from the XRD diffractograms. The micrographs at same magnification are shown in Figure 4.7 Accordingly, for the sample obtained after 12 hours of hydration (top image), the results align with the XRD diffractogram peaks shown in Figure 4.8. Flake-like CDHAp crystals can be observed, however some unreacted  $\alpha$ -TCP were still present. Therefore, it can be concluded that 12 hours of hydration is insufficient for complete conversion to CDHAp, Upon examination of the SEM micrographs corresponding to the 24-hour and 56-hour hydration periods, (middle and bottom images), fully reticulated structures-CDHAp-are observed. Specifically, the SEM image from the 56-hour hydration (Figure 4.7 bottom image) reveals signs of coarsening, with relatively larger plates/flakes. In can be said that SEM analyses are in agreement with the XRD findings, even though absolute specific times for start/completion times for  $\alpha$ -TCP  $\rightarrow$  HAp conversion can be determined, it can be roughly estimated.

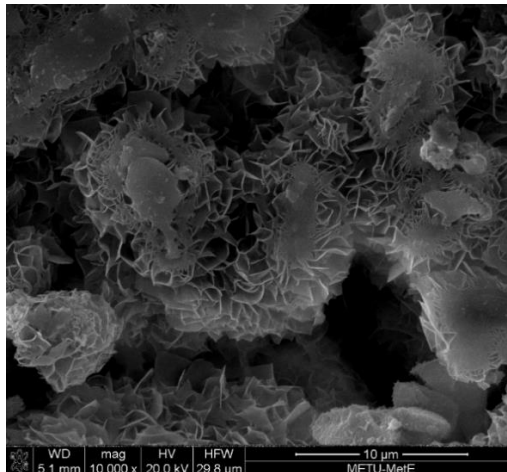
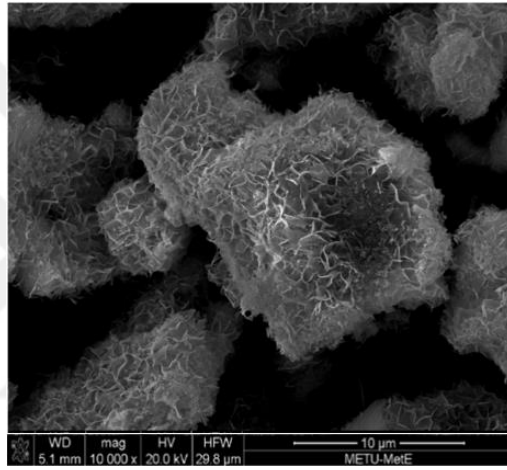
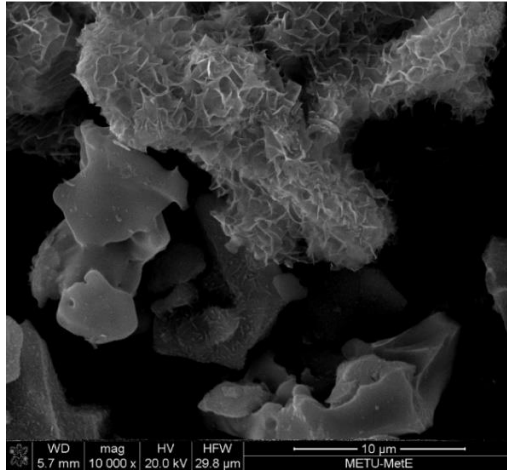


Figure 4.7 SEM micrographs of the product phase resulting from  $\alpha$ -TCP hydration at 37 °C with DI-water, for 12, 24, 56, hours respectively; (from top to bottom) with a s:l ratio of 1:3.

#### 4.5 Evaluation of hydration behavior of $\alpha$ -TCP: Hydration temperature

In the third set experimental studies this time another experimental hydration/reaction parameter, *reaction temperature*, on  $\alpha$ -TCP  $\rightarrow$  HAp conversion has been examined. As cement conversion occurs by a thermally activated dissolution and re-precipitation reaction, one can guess that temperature would be an obvious regulating factor. The reason for employing 37 °C as a typical reaction temperature so far was, to study hydration behavior simulating the real reaction environment, i.e. physiological environment. Again, XRD and SEM were the two main analytical tools used in this part.

The effect of temperature on  $\alpha$ -TCP hydration was examined, using a 1:3 solid-to-liquid ratio cement mixture, for 24 hours. The free  $\alpha$ -TCP powders were hydrated for 25°C, 37°C, and 60°C, enclosed in plastic vials with DI-water, merged/floated in constant temperature water bath.

The XRD data for hydrated samples are shown in Figure 4.8. XRD peaks corresponding to  $\alpha$ -TCP powders are still present after hydration at 25°C. While the diffractogram indicates that CDHAp transformation has started. It is evident that a hydration temperature of 25°C is insufficient for complete transformation within the 24-hour hydration period. In contrast to 25°C,  $\alpha$ -TCP powders hydrated at 37°C were fully converted to CDHAp. In this case, no peaks corresponding to  $\alpha$ -TCP were observed, and no peaks for any other calcium phosphate phases were detected. It can be concluded that a hydration temperature of 37°C, combined with a 24-hour duration and a 1:3 solid-to-liquid ratio, is sufficient for complete CDHAp conversion. It can be inferred that a hydration temperature of 60°C, similar to that hydrated at 37°C, is also sufficient for the complete conversion of  $\alpha$ -TCP powders to CDHAp. The slight differences in diffraction peak characteristics for samples hydrated different temperatures give an indirect about the crystal properties of resulting CDHAp. The peak shape and form for high temperature-hydrated samples, i.e. 37° and 60 °C is somewhat better and well-defined, suggesting relatively highly

crystalline nature of the resultant CDHAp. As it can be seen from the bottom diffractogram, the shoulder neighboring to the main 3-diffraction peaks ( $2\theta = 31^\circ$ - $33^\circ$  range), as well as splitting of these peaks for 37 C-hydrated samples seem to be little noisy compared the other two patterns.

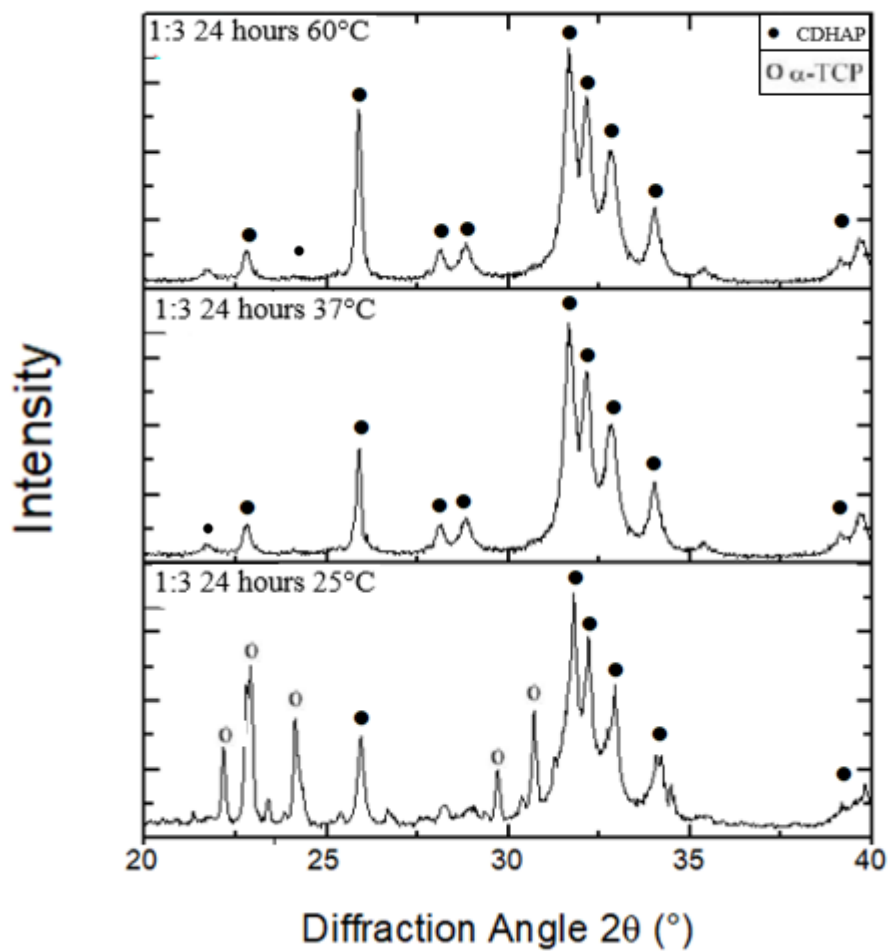


Figure 4.8 XRD diffractograms for hydrated products resulting from  $\alpha$ -TCP hydration with DI-water for 24 hours at 25, 37, 60  $^\circ$ C, respectively, with a s:l ratio of 1:3.

Accompanying SEM analyses are represented in Figure 4.9. The micrographs provided more insights about the effect of different hydration temperatures on microstructure and morphology of the resultant CDHAp cement products. These images are captured at the same magnification and relatively high magnification (x50000). The top figure is for the  $\alpha$ -TCP powders hydrated at 25°C, exhibiting a relatively different HAp morphology with needle crystals, instead previously shown plate/flake form. The product crystals are also not that much entangled/integrated. Samples hydrated at higher temperatures; 37 °C (middle image) and 60 °C (bottom image) on the other hand, exhibit the typical expected inter locked plate/flaky form resultant HAp crystal. The suggest that, even though HAp formation proceeds (at a limited extent according XRD) at 25 °C, the cement-type setting, hardening seem to be not occurring at low temperature. The hardening seems to produced microstructural effect, rather than a chemical change according to  $\alpha$ -TCP  $\rightarrow$  HAp. Setting occurs by interlocking of the crystal plates, somewhat isolated needle-like CDHAp crystals, most likely will produce a cement hardening.

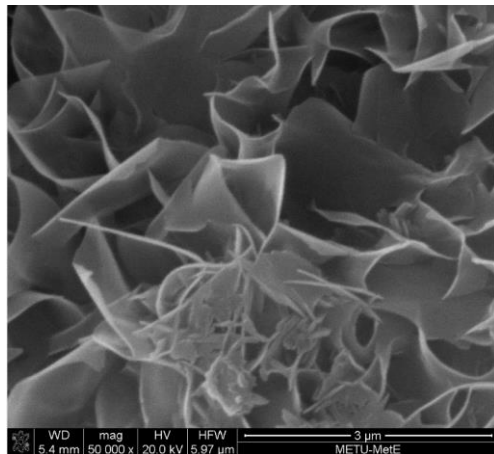
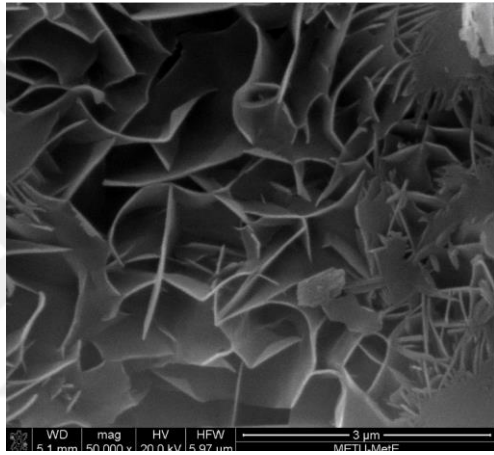
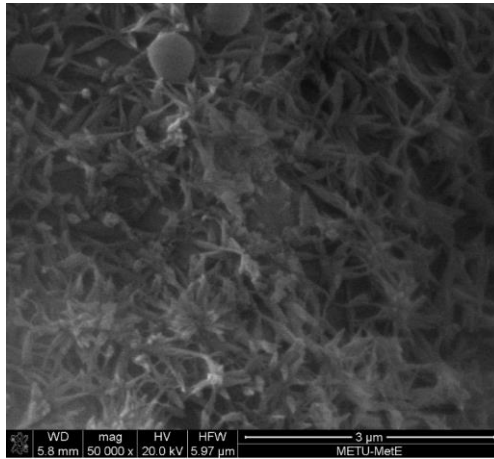


Figure 4.9 SEM micrographs of the product phase resulting from  $\alpha$ -TCP hydration with DI-water for 24 hours at 25, 37, 60 °C, respectively,(figure a,b,c from top to bottom), with a s:l ratio of 1:3.

#### 4.6 Evaluation of hydration behavior of $\alpha$ -TCP: Hydration media ( $\text{Na}_2\text{HPO}_4$ )<sub>aq</sub>

Finally, *the effect of hydration media*, on  $\alpha$ -TCP  $\rightarrow$  HAp conversion has been examined. For this purpose, an aqueous ionic solution of  $\text{Na}_2\text{HPO}_4$  has been used instead of DI-water. The reason of choosing this salt solution, was to examine the effects of a common ion, here  $(\text{PO}_4)^{3-}$ , on hydration kinetics and on physical/microstructural properties of CDHAp cement product. A common ion was expected to accelerate the conversion, as it can already provide ions, which are chemical constituents of HAp. In this case CDHAp formation can start without the need of dissolution of  $\alpha$ -TCP, providing these ions from the very beginning. Some experimental parameters, such as solid-to-liquid ratio (was set at 1:3), and hydration temperature ( $37^\circ\text{C}$ ) have been preset during these studies. Mainly the effect of ionic strength of  $\text{Na}_2\text{HPO}_4$  solution on hydration kinetics and on microstructure was explored. The hydration media were  $\text{Na}_2\text{HPO}_4$  solutions of variable concentration 1 wt. %, 2.5 wt. %, 5.0 wt. %.

The first analyses tool was again XRD. Figure 4.10 show the XRD diffractograms of hydrated samples using the three, 1 wt. %, 2.5 wt. %, 5.0 wt. %  $\text{Na}_2\text{HPO}_4$  solutions. Hydration efficiency remarkably changes due to use of  $\text{Na}_2\text{HPO}_4$ , as well as with concentration of the solution. The XRD peaks of the product formed after the hydration with 1 wt%  $\text{Na}_2\text{HPO}_4$  for 1 hour and 24 hours, are presented in Figure 4.16. According to the XRD diffractogram, the conversion of the  $\alpha$ -TCP powders to CDHAp did not occur after 1 hour of hydration. It is difficult to confirm when the conversion begins, as the characteristic peaks of  $\alpha$ -TCP remain after 1 h. However, after 24 hours of hydration period, it is clear that the complete conversion to CDHAp takes place.

The  $\alpha$ -TCP powders, hydrated with DI water containing 2.5 wt%  $\text{Na}_2\text{HPO}_4$  were subjected to hydration for durations of 5, 12, and 24 hours. XRD analysis of the samples revealed that the conversion to CDHAp commenced after both the 5 hours.

However, the characteristic XRD peaks corresponding to  $\alpha$ -TCP were still present, for 5h- and 12h-samples, indicating that the transformation was not yet complete. As a result, it is not possible to definitively evaluate the full effect of  $\text{Na}_2\text{HPO}_4$  addition during these shorter hydration times. In contrast, after a 24-hour hydration period, the conversion of  $\alpha$ -TCP to CDHAp was achieved, as evidenced by the complete disappearance of  $\alpha$ -TCP peaks and the emergence of peaks characteristic of CDHAp.

Finally, the phase analysis of  $\alpha$ -TCP powders hydrated with a 5 wt%  $\text{Na}_2\text{HPO}_4$  solution for 5, 12, and 24 hours is presented in Figure 4.16. Upon examining the XRD peaks, it is evident that the transformation of  $\alpha$ -TCP powders to CDHAp has completed in 12 hours. This is shorter than DI-water (part 4.4 of the thesis), and 1 and 2.5 wt %  $\text{Na}_2\text{HPO}_4$  solutions. In all these systems complete conversion takes 24 hours. This finding suggest that %  $\text{Na}_2\text{HPO}_4$  addition at certain amount accelerates the hydration process, a conclusion that is consistent with previously reported studies. [66].

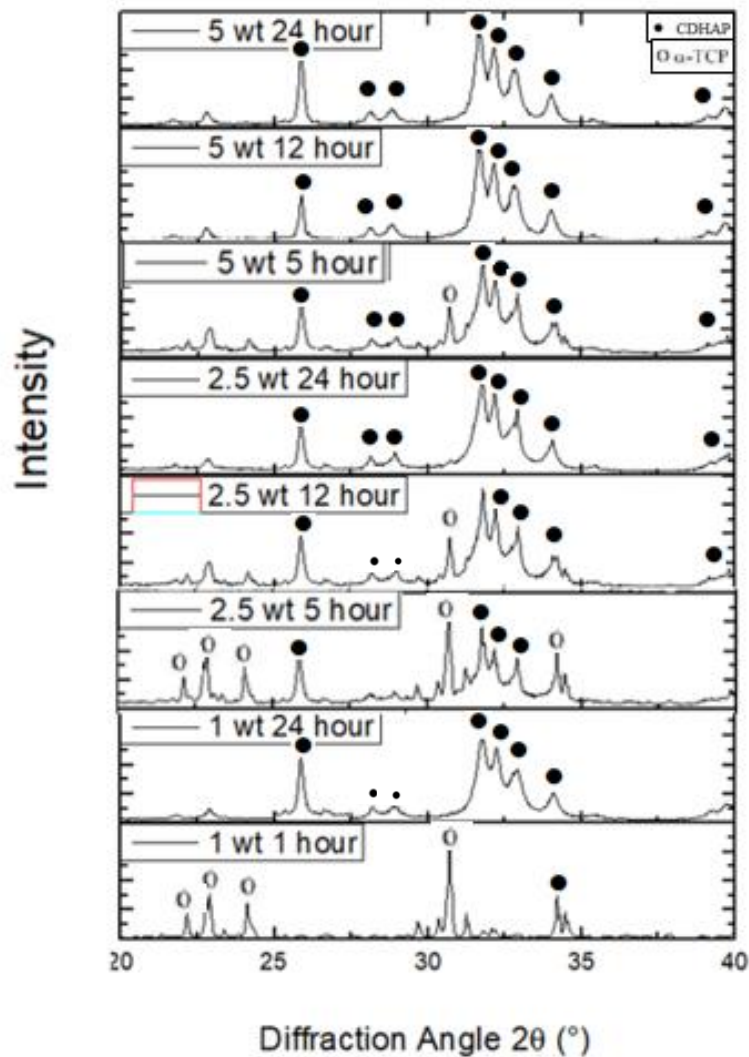


Figure 4.10. XRD diffractograms for hydrated products resulting from  $\alpha$ -TCP hydration in %  $\text{Na}_2\text{HPO}_4$  solutions (1.0 wt %, 2.5 wt% and 5.0 wt% ) at 37°C.

In addition, microstructural investigations have been conducted to examine the effect of hydration media on cement conversion. The micrographs, in Figure 4.11, offer additional insights into the impact of various hydration media on the microstructure and morphology of the resultant CDHAp cement products. These images were captured at the same magnification and a relatively higher magnification ( $\times 50,000$ ).

The top figure is for the  $\alpha$ -TCP powders hydrated with 1wt%  $\text{Na}_2\text{HPO}_4$ , exhibiting a relatively different HAp morphology with lack of needle crystals, instead previously shown plate/flake form. The product crystals are also not that much entangled/integrated. Samples hydrated with 2.5wt%  $\text{Na}_2\text{HPO}_4$  (middle image) and 5wt%  $\text{Na}_2\text{HPO}_4$  (bottom image) on the other hand, exhibit again needle like somewhat isolated CDHAp crystals. In these images, the amount of needle-like structures is notably higher compared to the 1 wt% image. However, the characteristic interlocked plate-like or flaky forms, which are typically observed, are not present.

Based on the XRD analysis, it can be concluded that the transformation is complete, and the final CDHAp product has been obtained. However, the SEM analysis reveals that a tightly bonded, homogeneously integrated structure is not observed at the microstructural level. Therefore, it can be inferred that structurally much better CDHAp cement products (hardened) are achieved when DI water is used exclusively as the hydration medium.

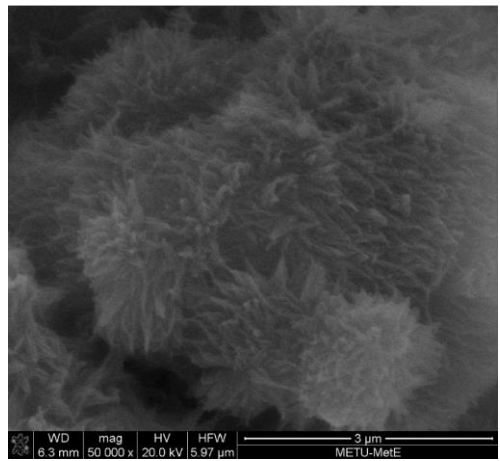
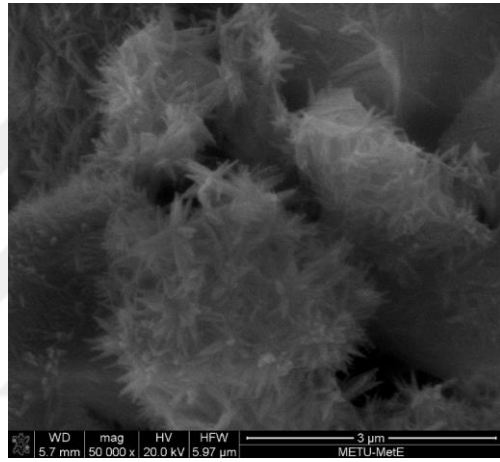
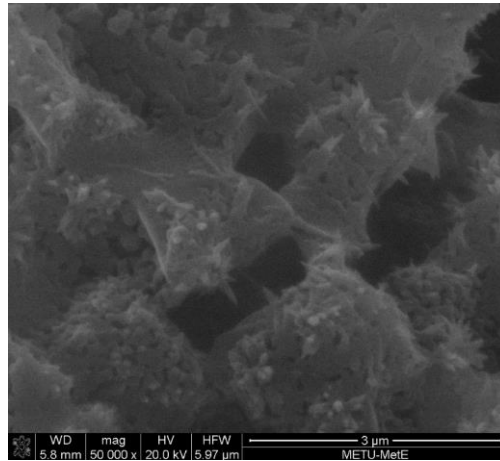


Figure 4.11. SEM micrographs of the product phase resulting from  $\alpha$ -TCP hydration with  $\text{Na}_2\text{HPO}_4$  solutions 1.0 wt %, 2.5 wt% and 5.0 wt% respectively (figure a,b,c from top to bottom) at  $37^\circ\text{C}$  for 24 hours.

#### 4.7 Evaluation of cement hardening: Mechanical testing

The mechanical properties of the product obtained from the hydration of  $\alpha$ -TCP powders, which were hydrated in pellet form using the method outlined in the pellet preparation section of Chapter 3, were evaluated. The diametral compressive strength values of different samples are presented in Figure 4.12. The strength will be referred as compressive strength just for simplicity, as the loading conditions in the diametral compression in fact leads to a fracture in tensile mode.

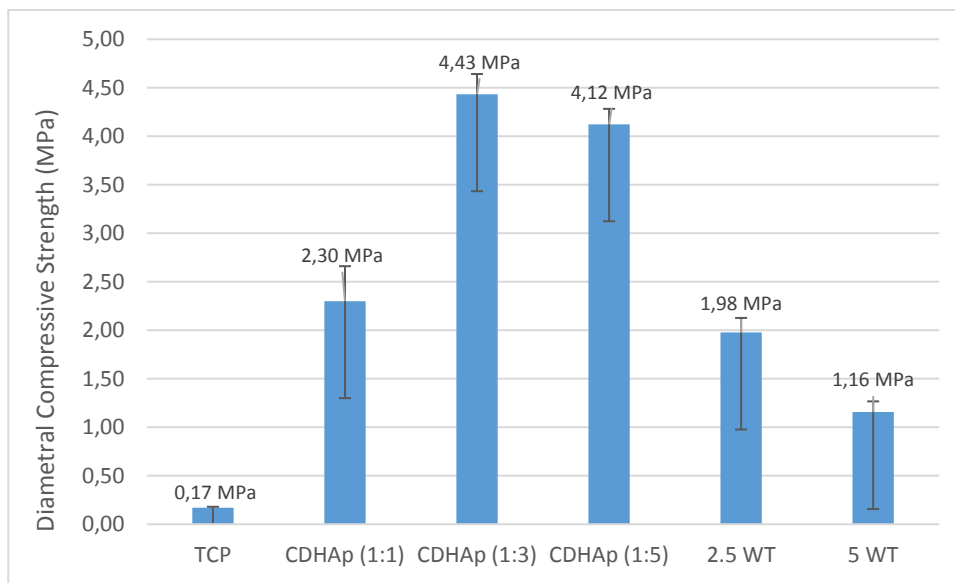


Figure 4.12. Mechanical properties of pure  $\alpha$ -TCP and  $\alpha$ -TCP pellets hydrated with DI water and  $\text{Na}_2\text{HPO}_4$  solutions, at varying solid-to-liquid ratios, at 37°C for 24 hours.

Some conclusions can be drawn from the data in Figure 4.12 in regard to the influence of various hydration parameters on the mechanical properties of the cement product. The compressive strength of the bare/unreacted  $\alpha$ -TCP pellet was found to be  $0.17 \pm 0.01$  MPa. This strength is just due to compaction of the free powder into a pellet compact form by pressing, it is not an absolute value for the strength of  $\alpha$ -TCP. This can be considered as reference mark. Meanwhile, the compressive strength of the CDHAp product, which was hydrated with DI water at a 1:1 solid-to-liquid ratio, shows an increase, with compressive strength of

approximately  $2.30 \pm 0.36$  MPa, indicating an somewhat effective cement-type hardening. The compressive strength of the CDHAp product, obtained using higher amount of water,  $\alpha$ -TCP pellets hydrated with at a solid-to-liquid ratio of 1:3, was measured at  $4.43 \pm 0.2$  MPa. Similarly, the strength of the product hydrated at a solid-to-liquid ratio of 1:5 was higher than of solid-to-liquid ratio 1:1, the compressive strength was determined as  $4.12 \pm 0.16$  MPa.

It is obvious that increase in the water amount leads to a significant enhancement in the mechanical properties. Upon comparison of the solid-to-liquid ratios of 1:1, 1:3, and 1:5, noteworthy insights regarding the influence of the solid-to-liquid ratio on the mechanical properties have emerged. Initially, when the mechanical properties corresponding to the 1:1 ratio are compared with those of the 1:3 and 1:5 ratios, a significant lower mechanical strength value was observed.

Furthermore, when 1:3 and 1:5 solid-to-liquid ratio samples are compared, slightly superior mechanical properties were obtained for the 1:3 ratio sample. However, this difference is marginal and is within the standard deviation values of the measurements. Such small difference does not provide a direct evidence to suggest that an excessive increase in the liquid content, i.e 1:5, adversely affects the mechanical properties. In conclusion, it can be inferred that an increase in the liquid ratio (beyond 1:1 ratio) definitely leads to an enhancement in the mechanical properties.

The examination of the microstructures corresponding to the 1:1, 1:3, and 1:5 ratios further supports this finding. In the microstructure of the 1:1 ratio, limited formation flake-like entangled structures were observed (Figure 4.5.). In contrast, the microstructures of the 1:3 and 1:5 ratios exhibited nearly complete formation of flake-like entangled structures in the final product (Figure 4.5.).

The effect of changes in the hydration media on mechanical properties was also investigated. In this regard,  $\text{Na}_2\text{HPO}_4$ -DI water solutions at concentrations of 2.5 wt. % and 5 wt.%, which were found to be accelerating hydration, were used during hydration of pellets. As shown in Figure 4.12, the use of  $\text{Na}_2\text{HPO}_4$  solution at both the 2.5 wt. % and 5 wt. % concentrations had an adverse impact on the mechanical properties. Specifically, the compressive strength for the 2.5 wt% ratio was only  $1.98 \pm 0.15$  MPa, while for the 5 wt% ratio, it was obtained as  $1.16 \pm 0.11$  MPa. These results suggest that the use of  $\text{Na}_2\text{HPO}_4$  solutions negatively affects the mechanical properties of the product.

The observed phenomenon can be attributed to the microstructural characteristics. The addition of  $\text{Na}_2\text{HPO}_4$  resulted in the formation of needle-like and somewhat loose clustered CDHAp crystals, which were not entangled with one another (Figure 4.11). In sum,  $\text{Na}_2\text{HPO}_4$  solutions accelerated the conversion of  $\alpha$ -TCP to CDHAp; however, they did not promote the formation of a proper cement microstructure exhibiting a hardening effect, i.e. plate/flake-like crystals that were integrated with each other.

## CHAPTER 5

### CONCLUSIONS

$\alpha$ -tricalcium phosphate ( $\alpha$ -TCP) was synthesized using the solid-state synthesis method, employing appropriate inorganic precursors. The transformation of this cement-type calcium phosphate reactant, to CDHAp, has been investigated by varying reaction parameters, including solid-to-liquid ratio, hydration time, hydration temperature, and hydration medium. The cement-type reactivity of the synthesized  $\alpha$ -TCP powders, particularly the transformation from  $\alpha$ -TCP to the final hardened product, calcium-deficient hydroxyapatite (CDHAp), was systematically studied. The effects of  $\text{Na}_2\text{HPO}_4$  as an alternative hydration medium was also evaluated. The structural characteristics of both  $\alpha$ -TCP and the end product, CDHAp, were examined using a range of complementary analytical characterization techniques. Finally, the mechanical properties of the cements were explored both before and after hydration process, taking some of the above mentioned experimental reaction parameters into account.

#### **Synthesis of $\alpha$ -TCP and evaluation of its' cement characteristics**

- $\alpha$ -TCP was successfully synthesized as pure, single-phase material via a solid-state reaction between monetite and calcium carbonate precursors.
- The parameters of solid-to-liquid ratio, hydration temperature, hydration time, and hydration medium were considered as variables, and their effects on the hydration process were analyzed in terms of phase composition, microstructure, and mechanical properties.
- The results demonstrated that solid-to-liquid mixtures with ratios of 1:3 and 1:5 yielded the most favorable outcomes, both in terms of phase formation and microstructural development.

- It was found that a temperature of 25°C was insufficient to achieve complete conversion, whereas hydration at both 37°C and 60°C resulted in successful conversion.
- Hydration in DI-water was observed to begin at 8 and 12 hours; however, complete conversion was not achieved until 24, at which point  $\alpha$ -TCP fully transformed to calcium-deficient hydroxyapatite (CDHAp).

#### **Evaluation of hydration behavior of $\alpha$ -TCP: Hydration media $(\text{Na}_2\text{HPO}_4)_{\text{aq}}$**

- In order to investigate the effects of different hydration media on the hydration of  $\alpha$ -tricalcium phosphate ( $\alpha$ -TCP), solutions were prepared by mixing sodium hydrogen phosphate ( $\text{Na}_2\text{HPO}_4$ ) with deionized (DI) water at concentrations of 1 wt%, 2.5 wt%, and 5 wt%.
- The results indicated that complete conversion of  $\alpha$ -TCP occurred in all samples hydrated for 24 hours with the 1 wt%, 2.5 wt%, and 5 wt%  $\text{Na}_2\text{HPO}_4$  concentrations.
- Notably, the addition of 5 wt%  $\text{Na}_2\text{HPO}_4$  reduced the required hydration time to 12 hours. Microstructural analysis revealed the formation of needle-like CHAp crystals after hydration, when  $(\text{Na}_2\text{HPO}_4)_{\text{aq}}$  were employed as hydration media.

#### **Evaluation of mechanical properties of $\alpha$ -TCP and hydration product**

- To evaluate the mechanical properties,  $\alpha$ -tricalcium phosphate ( $\alpha$ -TCP) and its hydration products were fabricated as pellets and subjected to compressive strength testing.

- The hydration products, prepared in molar ratios of  $\alpha$ -TCP to water of 1:1, 1:3, and 1:5, were hydrated for 24 hours at 37°C. Additionally, final products were hydrated using aqueous solutions of sodium hydrogen phosphate ( $\text{Na}_2\text{HPO}_4$ ) at concentrations of 2.5 wt% and 5 wt%.
- The test results indicated that the presence of  $\text{Na}_2\text{HPO}_4$  in the hydration mixture led to a reduction in mechanical strength. Among the different solid-to-liquid ratios, the highest compressive strength values were observed in the hydration products with ratios of 1:3 and 1:5.





## REFERENCES

- [1] Park, J. and Lakes, R. S. *Biomaterials: An introduction: Third edition.* (2007).
- [2] Weiner, S. and Wagner, H. D. "The Material Bone: Structure-Mechanical Function Relations," *Annu. Rev. Mater. Sci.*, 28, 271–298 (1998).
- [3] Currey, J. D. (2012). The structure and mechanics of bone. In *Journal of Materials Science* (Vol. 47, Issue 1, pp. 41–54). <https://doi.org/10.1007/s10853-011-5914-9>
- [4] Olszta, M. J., Cheng, X., Jee, S. S., Kumar, R., Kim, Y. Y., Kaufman, M. J., Douglas, E. P., & Gower, L. B. (2007). Bone structure and formation: A new perspective. In *Materials Science and Engineering R: Reports* (Vol. 58, Issues 3–5, pp. 77–116). <https://doi.org/10.1016/j.mser.2007.05.001>
- [5] Rho, J.-Y., Kuhn-Spearing, L., & Zioupos, P. (1998). Mechanical properties and the hierarchical structure of bone. In *Medical Engineering & Physics* (Vol. 20).
- [6] Safadi, F. F., Barbe, M. F., Abdelmagid, S. M., Rico, M. C., Aswad, R. A., Litvin, J., & Popoff, S. N. (2009). Bone structure, development and bone biology. In *Bone Pathology* (pp. 1–50). Humana Press. [https://doi.org/10.1007/978-1-59745-347-9\\_1](https://doi.org/10.1007/978-1-59745-347-9_1)
- [7] Weiner, S., & Wagner, H. D. (1998). THE MATERIAL BONE: Structure-Mechanical Function Relations. In *Annu. Rev. Mater. Sci* (Vol. 28).

[8] Zimmermann, E. A., & Ritchie, R. O. (2015). Bone as a Structural Material. In *Advanced Healthcare Materials* (Vol. 4, Issue 9, pp. 1287–1304). Wiley-VCH Verlag. <https://doi.org/10.1002/adhm.201500070>

[9] Reznikov, N., Shahar, R. and Weiner, S. “Bone hierarchical structure in three dimensions,” *Acta Biomater.*, 10, 3815–3826 (2014).

[10] Wang, Y. et al. “The predominant role of collagen in the nucleation, growth, structure and orientation of bone apatite,” *Nat. Mater.*, 37, 112–116 (2012).

[11] Rho, J., Kuhn-Spearing L. and Zioupos P., “Mechanical properties and the hierarchical structure of bone Jae-Young,” *Med. Eng. Phys.*, 92, 92–102 (1998).

[12] Kuhn-Spearing L, G. M., Rey C., Kim, H.M. “Carbonated apatite nanocrystals of bone. Synthesis and processing of nanocrystalline powder,” *Miner. Met. Mater. Soc.* (1996).

[13] Yusufoglu, Y. “Synthesis and characterization of carbonated hydroxyapatite and bioinspired polymer-calcium phosphate nanocomposites,” (2009).

[14]Burger, C. et al., “Lateral Packing of Mineral Crystals in Bone Collagen Fibrils,” *Biophys. J.*, 95, 1985–1992 (2008).

[15]Dorozhkin, S. V. “Biocomposites and hybrid biomaterials based on calcium orthophosphates,” 2535 (2011).

[16]Ana, I. D., Satria, G. A. P., Dewi, A. H., & Ardhani, R. (2018). *Bioceramics for Clinical Application in Regenerative Dentistry*. In *Advances in Experimental Medicine and Biology* (Vol. 1077, pp. 309–316). Springer New York LLC.  
[https://doi.org/10.1007/978-981-13-0947-2\\_16](https://doi.org/10.1007/978-981-13-0947-2_16)

[17]Best, S. M., Porter, A. E., Thian, E. S., & Huang, J. (2008). *Bioceramics: Past, present and for the future*. *Journal of the European Ceramic Society*, 28(7), 1319–1327. <https://doi.org/10.1016/j.jeurceramsoc.2007.12.001>

[18]El-Ghannam, A. (2005). *Bone reconstruction: From bioceramics to tissue engineering*. In *Expert Review of Medical Devices* (Vol. 2, Issue 1, pp. 87–101). Future Drugs Ltd. <https://doi.org/10.1586/17434440.2.1.87>

[19] Ginebra, M. P., Espanol, M., Maazouz, Y., Bergez, V., & Pastorino, D. (2018). *Bioceramics and bone healing*. *EFORT Open Reviews*, 3(5), 173–183.  
<https://doi.org/10.1302/2058-5241.3.170056>

[20]Hench, L. L. (2015). *The future of bioactive ceramics*. *Journal of Materials Science: Materials in Medicine*, 26(2). <https://doi.org/10.1007/s10856-015-5425-3>

[21]Kumar, A., Goyal, A., Manhas, S., Kumar, D., Kumar, A., & Sharma, A. (2022). Trends, technology, and future prospects of bioceramic materials. In *Advanced Ceramics for Versatile Interdisciplinary Applications* (pp. 251–277). Elsevier. <https://doi.org/10.1016/B978-0-323-89952-9.00017-8>

[22]Pina, S., Rebelo, R., Correlo, V. M., Oliveira, J. M., & Reis, R. L. (2018). Bioceramics for Osteochondral Tissue Engineering and Regeneration. In *Advances in Experimental Medicine and Biology* (Vol. 1058, pp. 53–75). Springer New York LLC. [https://doi.org/10.1007/978-3-319-76711-6\\_3](https://doi.org/10.1007/978-3-319-76711-6_3)

[23]Thamaraiselvi, T. v, & Rajeswari, S. (2004). Biological Evaluation of Bioceramic Materials-A Review. In *Trends Biomater. Artif. Organs* (Vol. 18, Issue 1).

[24]Vallet-Regí, M. (2010). Evolution of bioceramics within the field of biomaterials. In *Comptes Rendus Chimie* (Vol. 13, Issues 1–2, pp. 174–185). <https://doi.org/10.1016/j.crci.2009.03.004>

[25]Washio, A., Morotomi, T., Yoshii, S., & Kitamura, C. (2019). Bioactive Glass-Based Endodontic Sealer as a Promising Root Canal Filling Material without Semisolid Core Materials. *Materials*, 12(23), 3967. <https://doi.org/10.3390/ma12233967>

[26]Wilson, E. E., Awonusi, A., Morris, M. D., Kohn, D. H., Tecklenburg, M. M. J. and Beck, L. W. “Three structural roles for water in bone observed by solid- state NMR,” *Biophys. J.*, 90, 3722–3731 (2006).

[27] Lieberman, J. R. and Friedlaender, G. E. Bone regeneration and repair: biology and clinical applications. Humana Press (2005).

[28] Vaccaro, A. R. et al., “Bone grafting alternatives in spinal surgery,” *Spine J.*, 2, 206–215 (2002).

[29] Moore, W. R., Graves, S. E. and Bain, G. I. “Synthetic Bone Graft Substitutes,” 354–361 (2001).

[30] Albrektsson T. and Johansson C. “Osteoinduction, osteoconduction and osseointegration,” *Eur. Spine J.*, 10, S96–S101 (2001).

[31] Kelly, C. M., Wilkins, R. M., Gitelis, S., Hartjen, C., Watson, J. T. and Kim, P. T. “The Use of a Surgical Grade Calcium Sulfate as a Bone Graft Substitute,” *Clin. Orthop. Relat. Res.*, 382, 42–50 (2001).

[32] Singh, N. B. and Middendorf, B. “Calcium sulphate hemihydrate hydration leading to gypsum crystallization,” *Prog. Cryst. Growth Charact. Mater.*, 53, 57–77 (2007).

[33] Hu, G., Xiao, L., Fu, H., Bi, D., Ma, H. and Tong, P. “Study on injectable and degradable cement of calcium sulphate and calcium phosphate for bone repair,” *J. Mater. Sci. Mater. Med.*, 21, 627–634 (2010).

[34] Dorozhkin, S. V. “Calcium Orthophosphates as Bioceramics: State of the Art,” *J. Funct. Biometer.*, 1, 22–107 (2010).

- [35] Albee F. H. and Morrison, H. F. "Studies in Bone Growth: triple calcium phosphate as a stimulus osteogenesis," *Ann. Surg.*, 71, 32–39 (1920)
- [36] Ray, R., Degge, J., Gloyd, P. and Mooney, G. "Bone regeneration," *J. Bone Jt. Surg.*, 638–647 (1952).
- [37] .Bohner, M. "Calcium orthophosphates in medicine: From ceramics to calcium phosphate cements," *Injury*, (2000).
- [38] Dorozhkin, S. V. "Self-Setting Calcium Orthophosphate Formulations," *J. Funct. Biomater.*, 4, 209–311 (2013).
- [39] Dorozhkin, S. V. "Bioceramics of calcium orthophosphates," *Biomaterials*, 31, 1465–1485 (2010).
- [40] Jarcho, M., Bolen, C. H., Thomas, M. B., Bobick, J., Kay, J. F. and Doremus, R. H. "Hydroxylapatite synthesis and characterization in dense polycrystalline form," *J Mater Sci*, 11, 2027–2035 (1976).
- [41] De Groot, K. "Bioceramics consisting of calcium phosphate salts," *Biomaterials*, 1, 47–50 (1980).
- [42] Akao, M, Aoki, H. and Kato, K. "Mechanical properties of sintered hydroxyapatite for prosthetic applications," *J. Mater. Sci. Mater. Med.*, 16, 809–812 (1981).

[43]Aaron Posner, B. S. (1958). Refinement of the hydroxyapatite structure.\*. In 308 SHORT COMMUNICATIONS Acta Cryst (Vol. 11).

[44]Bohner, M., Galea, L., & Doebelin, N. (2012). Calcium phosphate bone graft substitutes: Failures and hopes. *Journal of the European Ceramic Society*, 32(11), 2663–2671. <https://doi.org/10.1016/j.jeurceramsoc.2012.02.028>

[45]Diez-Escudero, A., Espanol, M., & Ginebra, M. P. (2023). High-aspect-ratio nanostructured hydroxyapatite: towards new functionalities for a classical material. In *Chemical Science* (Vol. 15, Issue 1, pp. 55–76). Royal Society of Chemistry. <https://doi.org/10.1039/d3sc05344j>

[46]Fox, K., Tran, P. A., & Tran, N. (2012). Recent advances in research applications of nanophase hydroxyapatite. *ChemPhysChem*, 13(10), 2495–2506. <https://doi.org/10.1002/cphc.201200080>

[47]Gallinetti, S., Canal, C., & Ginebra, M. P. (2014). Development and characterization of biphasic hydroxyapatite/ $\beta$ -TCP cements. *Journal of the American Ceramic Society*, 97(4), 1065–1073. <https://doi.org/10.1111/jace.12861>

[48]Gomes, D. S., Santos, A. M. C., Neves, G. A., & Menezes, R. R. (2019). A brief review on hydroxyapatite production and use in biomedicine. In *Ceramica* (Vol. 65, Issue 374, pp. 282–302). Associacao Brasileira de Ceramica. <https://doi.org/10.1590/0366-69132019653742706>

[49]Konka, J., Buxadera-Palomero, J., Espanol, M., & Ginebra, M. P. (2021). 3D printing of hierarchical porous biomimetic hydroxyapatite scaffolds: Adding concavities to the convex filaments. *Acta Biomaterialia*, 134, 744–759.

<https://doi.org/10.1016/j.actbio.2021.07.071>

[50]Legeros, R. Z., & Legeros, J. P. (2008). Hydroxyapatite. In *Bioceramics and their Clinical Applications* (pp. 367–394). Elsevier Inc.

<https://doi.org/10.1533/9781845694227.2.367>

[51] Pokhrel, S. (2018). Hydroxyapatite: Preparation, Properties and Its Biomedical Applications. *Advances in Chemical Engineering and Science*, 08(04), 225–240.

<https://doi.org/10.4236/aces.2018.84016>

[52]Szcześ, A., Hołysz, L., & Chibowski, E. (2017). Synthesis of hydroxyapatite for biomedical applications. In *Advances in Colloid and Interface Science* (Vol. 249, pp. 321–330). Elsevier B.V.

<https://doi.org/10.1016/j.cis.2017.04.007>

[53]Kohn, M., Rakovan, J. and Hughes, J. M. *Phosphates: geochemical, geobiological and materials importance*. Mineral Society of America, Washington, DC (2002).

[54]Dorozhkin, S. V. “Calcium orthophosphates,” *J. Mater. Sci.*, 42, 1061–1095 (2007).

[55]Dorozhkin, S. V. “Nanodimensional and nanocrystalline apatites and other calcium orthophosphates in biomedical engineering, biology and medicine,” *Materials* (Basel), 2, 1975–2045 (2009).

[56]Dorozhkin, S. V. “Calcium orthophosphates in nature, biology and medicine,” *Materials (Basel)*, 2, 399–498 (2009).

[57]Carrodeguas, R. G. and De Aza, S. “ $\alpha$ -Tricalcium phosphate: Synthesis, properties and biomedical applications,” *Acta Biomater.*, 7, 3536–3546 (2011).

[58]Nikaido, T. et al., “Fabrication of  $\beta$ -TCP foam: Effects of magnesium oxide as phase stabilizer on its properties,” *Ceram. Int.*, 41, 14245–14250 (2015).

[59]Ogose, A. et al., “Histological examination of  $\beta$ -tricalcium phosphate graft in human femur,” *J. Biomed. Mater. Res.*, 63, 601–604 (2002).

[60]Camiré, C. L., Saint-Jean, S. J., Hansen, S., McCarthy, I. and Lidgren, L. “Hydration characteristics of  $\alpha$ -tricalcium phosphates: Comparison of preparation routes,” *J. Appl. Biomater. Biomech.*, 3, 106–111 (2005).

[61]Bohner, M., Brunner, T. J., Doebelin, N., Tang, R. and Stark, W. J. “Effect of thermal treatments on the reactivity of nanosized tricalcium phosphate powders,” *J. Mater. Chem.*, 18, 4460–4467 (2008).

[62]Kitamura, M., Ohtsuki, C., Iwasaki, H., Ogata, S. I., Tanihara, M. and Miyazaki, T. “The controlled resorption of porous  $\alpha$ -tricalcium phosphate using a hydroxypropylcellulose coating,” *J. Mater. Sci. Mater. Med.*, 15, 1153–1158 (2004).

[63]Tronco, M. C., Cassel, J. B., & dos Santos, L. A. (2022).  $\alpha$ -TCP-based calcium phosphate cements: A critical review. In *Acta Biomaterialia* (Vol. 151, pp. 70–87). Acta Materialia Inc. <https://doi.org/10.1016/j.actbio.2022.08.040>

[64]Durucan, C., Brown, P.W. (2000). Calcium Deficient hydroxyapatite,PLGA composites: Mechanical and microstructural investigation. *Journal of Biomedical Materials Research* (Vol 51, Issue 4, pp. 726-734)

[65]Patrick Leamy, P. W. Brown, Kevor TenHuisen, et al. Fluoride uptake by hydroxyapatite formed by the hydrolysis of tricalcium phosphate. *Journal of Biomedical Materials Research*. 1998, Vol.42, No.3, p.458.

[66] Fulmer, M. T., & Brown, P. W. (1993). Effects of  $\text{Na}_2\text{HPO}_4$  and  $\text{NaH}_2\text{PO}_4$  on hydroxyapatite formation. *Journal of Biomedical Materials Research*